We are thankful to the two referees for their thoughtful and constructive comments which help improve the manuscript substantially. Following the reviewers' suggestions, we have revised the manuscript accordingly. Listed below are our point-by-point responses in blue to each comment that is repeated in italic.

Response to Reviewer #1

This is a very important and necessary piece of work comparing mass spectral profiles of different organic aerosol types comparing the 'standard' vs 'capture' vaporisers used in the AMS and ACSM. While it is acknowledged that there are differences between the two, an extensive comparison for different 'real world' aerosols is currently lacking. The experiments are appropriately and methodically performed and include both online and offline measurements, making these results applicable to both. This paper demonstrates the improvement to ME-2 source apportionment when these profiles are applied, showing this to be a very important technical contribution that will aid analysis in the future. While the aerosols sampled are undeniably focused on Chinese sources, given the number of these instruments in use in China currently, this will still be of much use to the community and is firmly within scope for AMT. The work is appropriately and methodically performed and generally well written. I have only a couple of minor comments, but otherwise recommend publication.

We thank the reviewer's comments and have revised the manuscript accordingly.

Data availability: Given the scope for utilisation of this data, I would strongly encourage the mass spectral profiles to be hosted on a public archive. Traditionally, this has been the University of Colorado database. One would expect that future utilisation of these profiles by others will drive up the paper's citations, so it will be in the authors' interests to do so.

We will do that after the manuscript was accepted.

Consider placing figures S1 and S2 in the main article, as I think these are of sufficient interest that they should exist there.

It is a good point. We moved these two figures from supplementary to the main text in the revised manuscript.

Page 2, line 14: Should be 'owing' rather than 'owining'

Changed

Response to Reviewer #2

This manuscript provides a comprehensive data set for the characterization of primary OAs using the CV-ACSM compared to the SV-AMS. Similar spectral characteristics were found between the SV-AMS and CV-ACSM, and the latter showed additional thermal decomposition in the spectra. There is another paper on AMTD that addresses the similar topic (https://www.atmos-meas-tech-discuss.net/amt-2019- 449/). This study should make comparisons to that one. Overall, the paper is well written. I recommend acceptance for publication on AMT after minor revisions.

We appreciate the reviewer for pointing out this important paper. The comparisons between two studies have been made in the revised manuscript.

"For example, the m/z 55/57 ratios ranged from 2.8 to 5.4 in CV-ACSM, which were consistent with those of cooking exhaust near a kitchen ventilator (4.05) measured by another similar CV-ACSM (Zheng et al., 2020), yet the ratios were approximately twice higher than those in SV-AMS (2.0 – 2.7, Fig. 6)."

"One reason is due to the high solubility of BBOA of which ~40 – 70% of carbon was found to be water-soluble. This is consistent with the observation from a combustion chamber experiment (65%) (Zheng et al., 2020). It should be noted that the f_{60} of WSBBOA measured by CV-ACSM in this study is higher than that reported in Zheng et al. (2020) likely due to the differences in combustion system and ACSM detectors."

"the PAHs signals are well retained in the mass spectra of CV-ACSM (e.g., m/z 152, m/z 165, m/z 178, m/z 189, m/z 202, m/z 215) due to the stabilized chemical structures that are very resistant to fragmentation after ionization (McLafferty and Turecek, 1993), consistent with the observations of PAHs from burning different types of coals (Zheng et al., 2020)."

Specific comments:

Page 3, Line 27: What kind of stove was used?

The common residential stove was used in this study. We added the description in the revised manuscript to clarify it (also shown in Figure 1).

Figure 1 is difficult to read especially for the standard deviations. I suggest to split Figure 1 to 2 graphs (one for OA and the other for WSOA) and enlarge the mass spectra.

This is a good suggestion. We split Figure 1 into two figures in the revised manuscript.

Page 5, Line 16-17: Please indicate what numbers were shown in the parentheses? I think you mean f60 and

f73. Has other COA studies also showed pronounced f60 and f73? Please compare. Also, what fuel was used for cooking? Is it possible that the signals of levoglucosan come from the burning of the fuel?

Thank the reviewer's comments. The number in the parentheses is f_{60} and f_{73}.

We expanded the discussions in the revised manuscript. Now it reads:

"We also noticed pronounced m/z 60 (f_{60}=0.57-0.96%) and m/z 73 (f_{73}=0.59-1.1%) in COA source spectra, which are generally used as biomass burning tracers (Cubison et al., 2011). Because an induction cooker was used in this study, the signals of f_{60} and f_{73} would be completely from cooking oils. Previous studies also observed such signals from laboratory-generated cooking emissions, for example, palm oil COA (Liu et al., 2018;Liu et al., 2017), fresh COA (Kaltsonoudis et al., 2017), heating of frying oil and deep-frying (Faber et al., 2013). Although the chemical ionization mass spectrometer was able to detect high concentrations of levoglucosan in cooking emissions (Reyes-Villegas et al., 2018a), the ratios of f_{60}/f_{73} in COA from SV-AMS are fairly constant (~1, Fig. 6), which are approximately twice lower than those observed in biomass burning OA (~2, Fig. 6). These results highlight the contributions of other cooking-related oxygenated compounds to m/z 60 and m/z 73."

We described the cooking styles in section 2.2. Now it reads:

Cooking experiments were conducted inside the tent by simulating the real Chinese cooking styles with different oils. To avoid the influences from burning of the fuel, an induction cooker was used in this study.

Page 5, Line 20-24: If the CV-ACSM sampled PM$_{2.5}$ and the SV-AMS sampled PM$_1$, there might be a composition difference. When comparing the two (not only for COA but also for other OAs), please justify the conclusions with that in mind.

Also, the authors mentioned about less enhancement of f44 compared to Hu et al. 2018a. Can this be partially explained by the loading difference? I mean the loadings herein were 2 orders of magnitude greater than ambient OA concentrations. More volatile species may partition to the particle phase compared to Hu et al. 2018a as well as the other study that I mentioned earlier. Please indicate the difference of conditions when making the comparisons.

We agree with the reviewer that there could be compositional difference between PM$_1$ and PM$_{2.5}$. In fact, a recent ambient study in north China indicated that the differences of primary OA between PM$_1$ and PM$_{2.5}$ were small even under high relative humidity conditions (Sun et al., 2020). In this work, the experiments were conducted during periods with relative humidity less than 60%, and the source spectra of primary OA

between PM_1 and $PM_{2.5}$ are not expected to be largely different. Most importantly, the size distributions of primary OA from AMS measurements showed that aerosol particles from burning different fuels were below 1 μm, supporting that the differences between PM_1 and $PM_{2.5}$ would not be important for this study.

Thanks for pointing out the loading effect on mass spectra. In fact, we compared f_{44} of OA from burning different fuels under different mass loadings (Figure R1). Indeed, f_{44} from biomass and wood burning overall showed relatively lower f_{44} during periods with higher mass loadings, likely due to partitioning of more semi-volatile organic compounds under higher mass loadings. In contrast, higher f_{44} for lower mass loadings could be due to the evaporation of semi-volatile organic compounds or rapid ageing of OA in the atmosphere. We clarified this in the revised manuscript with a new paragraph (see our response to the next comment).

"All COA spectral profiles measured by SV-AMS and CV-ACSM are highly similar ($R^2>0.89$, Fig. 5), and also resemble those previously resolved in ambient air during all seasons in Beijing (Fig. S4) despite the COA concentrations can have a difference of an order of magnitude. We also noticed slightly higher O/C (f_{44}) for COA under lower mass loadings, which were likely due to partitioning of more semi-volatile organics on particles during periods with higher mass loadings (Reyes-Villegas et al., 2018)."

"As shown in Figs. 3 and S6, all COA spectra of CV-ACSM are fairly stable and overall similar to those of SV-AMS ($R^2> 0.86$). Due to additional thermal decomposition in CV, the COA source spectra in CV showed slightly higher f_{44} (2.4–3.7%) than that of SV-AMS (1.8–2.9%)(Hu et al., 2018a)."
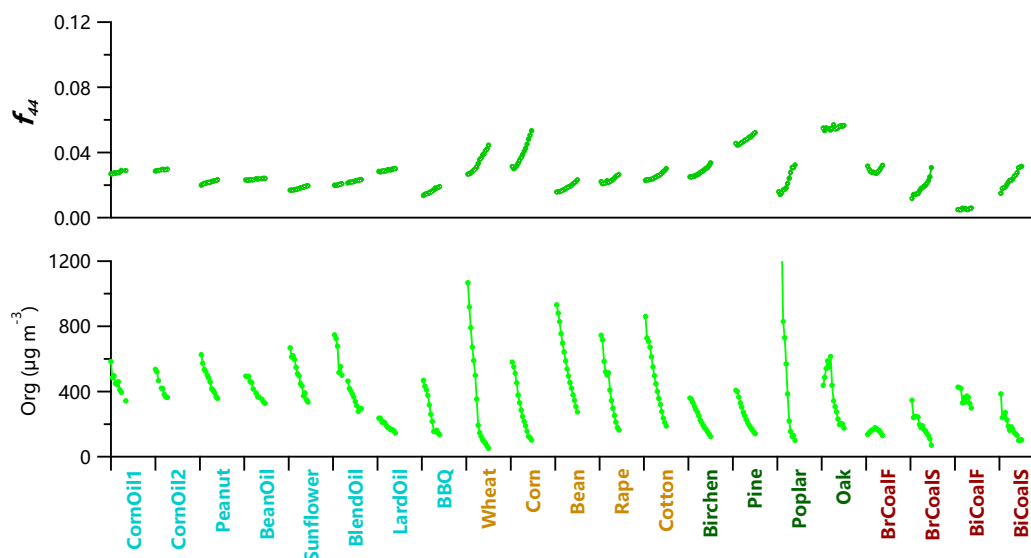

Figure R1. The variations of f_{44} and mass loadings of OA measured by SV-AMS in each experiment. The default RIE (1.4) and CE=1 were used.

Page 10, Line 6-7: The water-soluble fraction of POA also depends on the atmospheric dilution of the primary sources. This study should discuss about the sampling OA loading levels and the possible change of solubility after atmospheric dilution. Would that change the order of solubility?

Thanks for the reviewer's suggestion. The water-soluble fraction of POA in this study was estimated by the ratio of WSOC/OC with high mass loading. It should be noted that WSOA/OA ratio was also an indicator of water solubility in previous observations. The study of WSOC in Helsinki (Finland) and Paris (France) showed that 64% and 82% of the OC was water-soluble for wild land fires (Timonen et al., 2008) and wood burning (Sciare et al., 2011), respectively. By coupling a Particle-Into-Liquid-Sampler (PILS) and AMS, Xu et al. (2017) found that the average water solubility of BBOA was 75% with a large variation in southeastern America. The vertical distribution of WSOA sources in Beijing showed that 61 – 78% of BBOA was water-soluble at ground and 260 m level (Qiu et al., 2019). This discrepancy was likely due to the different biomass types and burning conditions. Similar to BBOA, the water-soluble fraction of COA also has a wide frequency distribution (8 – 40%)(Li et al., 2018). In additional, the water-solubility of COA estimated by combining online AMS and offline WSOA measurements was 19% at ground and 42% at 260 m in Beijing, this difference of COA water solubility was likely due to the ageing process associated with regional or vertical transport (Qiu et al., 2019). These results indicate that the order of water solubility of OA was unlikely changed due to the atmospheric dilution processes considering the large differences in water solubility for different primary OA.
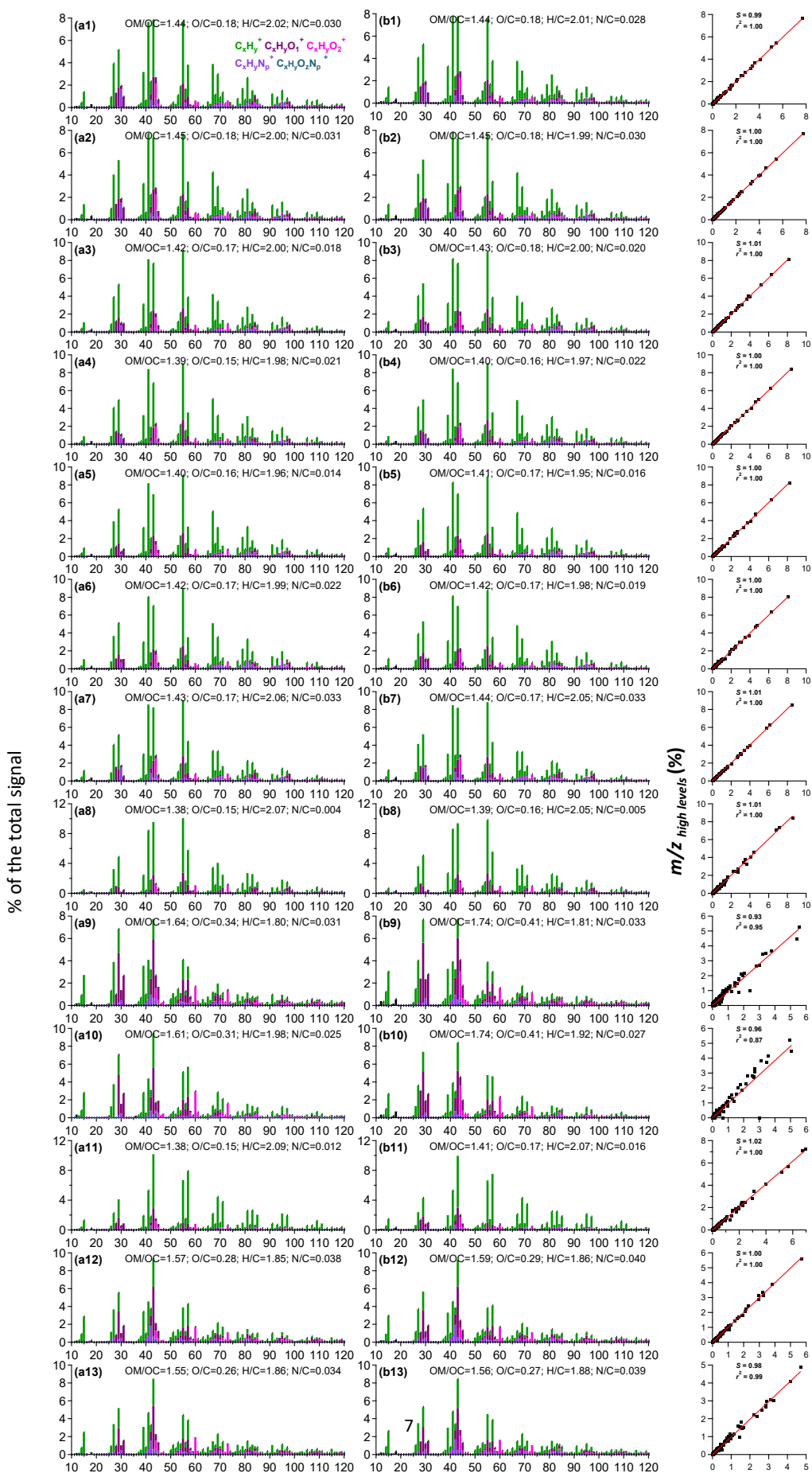
We expanded the discussions in the revised manuscript. Now it reads:

"However, the spectral differences between water-soluble OA and the total OA can be substantial for both SV-AMS and CV-ACSM depending on water solubility which is in the order of BBOA > WBOA > COA > CCOA. Noted that the mass loadings of primary emissions in this experiment are much higher than those in ambient air, which could cause some differences in water solubility and subsequent spectral differences in WSOA."

The loading-dependent OA composition also limits the application of the source profile directly in ME-2 (Page 10, Line 18-25). For example, if the source profile is obtained at 1000 ug m-3, the actual source in the atmosphere is indeed tens of ug m-3 after quick dilution. Many studies have shown the OA composition varied a lot at various loadings especially for combustion sources like BBOA and CCOA and hence may change the mass spectra. The authors should be clarify this complication and do not mislead users to use the source profiles without cautions.

This is really a good point we didn't discuss before. Following the reviewer's suggestions, we further compared the source spectra of OA between low and high mass loadings, and also the changes in f_{44} and f_{60}. We found that the mass spectra of COA and flaming combustion of coal are very stable across different mass loadings. Although the mass spectra of OA for the rest fuel burning are highly similar, the changes in f_{44} and f_{60} were also observed between low and high mass loadings. We then expanded the discussions on loading effects on mass spectra in the revised manuscript, and clarified the uncertainties that were caused by mass loadings. Now, the mass loadings for each burning experiment, and the comparisons of OA mass spectra between low and high mass loadings are all presented in supplementary (Figures S1 and S2, and Tables S1 and S2).

"The average mass loadings of OA during the burning and cooking experiments are nearly 2 order of magnitude of that in ambient air, indicating the negligible influences of background OA to our experiments. As shown in Table S1, the mass concentrations of OA measured by SV-AMS ranged from ~80 µg m^{-3} to ~1370 µg m^{-3} for different burning experiments by using a relative ionization efficiency of 1.4 and a collection efficiency of 1. Considering that the mass spectra of OA can have changes across different mass loadings due to the partitioning of semi-volatile organic compounds(Donahue et al., 2006; Shilling et al., 2009), we further checked the spectral differences between high and low mass loadings for SV-AMS and CV-ACSM (Tables S1 and S2, respectively). As indicated in Figures S1 and S2, the mass spectra of OA, and f_{44}, f_{43}, and f_{60} from cooking and flaming combustion of coal are remarkably similar under low and high mass loadings, indicating that the mass spectra are relatively stable upon dilution or evaporation, and thus can be well used as constraints in source apportionment analysis. Although the mass spectra of OA for the rest burning, i.e., biomass burning, wood burning, and smoldering combustion of coal are also highly similar between low and high mass loadings, the ubiquitous increases in f_{44} and corresponding decreases in f_{60} were observed from high to low mass loadings. For instance, f_{44} in SV-AMS was increased by $0.4 - 2\%$ as the mass loading decreased by a factor of ~3, and f_{60} showed a corresponding decrease by $0.1 - 0.9\%$. Similarly, f_{44} in CV-ACSM was increased by $0.9 - 4.2\%$ associated with a decrease in f_{60} by $0.1 - 0.6\%$ as OA mass loadings were decreased by a factor of $~3 - 4$. Such results are consistent with previous studies that biomass burning OA can be rapidly aged in the atmosphere which is characterized by increases in f_{44} and decreases in f_{60} (Cubison et al., 2011; Morgan et al., 2020). Therefore, source apportionment of OA using the source spectra from biomass burning, wood burning and smoldering combustion of coal need to consider the mass loading effect and increase the variability uncertainties in f_{44} and f_{60}. "

(a1) OM/OC=1.44; O/C=0.18; H/C=2.02; N/C=0.030

$C_xH_y^+$ $C_xH_yO_1^+$ $C_xH_yO_2^+$
$C_xH_yN_p^+$ $C_xH_yO_2N_p^+$

(b1) OM/OC=1.44; O/C=0.18; H/C=2.01; N/C=0.028
S = 0.99; r^2 = 1.00

(a2) OM/OC=1.45; O/C=0.18; H/C=2.00; N/C=0.031
(b2) OM/OC=1.45; O/C=0.18; H/C=1.99; N/C=0.030
S = 1.00; r^2 = 1.00

(a3) OM/OC=1.42; O/C=0.17; H/C=2.00; N/C=0.018
(b3) OM/OC=1.43; O/C=0.18; H/C=2.00; N/C=0.020
S = 1.01; r^2 = 1.00

(a4) OM/OC=1.39; O/C=0.15; H/C=1.98; N/C=0.021
(b4) OM/OC=1.40; O/C=0.16; H/C=1.97; N/C=0.022
S = 1.00; r^2 = 1.00

(a5) OM/OC=1.40; O/C=0.16; H/C=1.96; N/C=0.014
(b5) OM/OC=1.41; O/C=0.17; H/C=1.95; N/C=0.016
S = 1.00; r^2 = 1.00

(a6) OM/OC=1.42; O/C=0.17; H/C=1.99; N/C=0.022
(b6) OM/OC=1.42; O/C=0.17; H/C=1.98; N/C=0.019
S = 1.00; r^2 = 1.00

(a7) OM/OC=1.43; O/C=0.17; H/C=2.06; N/C=0.033
(b7) OM/OC=1.44; O/C=0.17; H/C=2.05; N/C=0.033
S = 1.01; r^2 = 1.00

(a8) OM/OC=1.38; O/C=0.15; H/C=2.07; N/C=0.004
(b8) OM/OC=1.39; O/C=0.16; H/C=2.05; N/C=0.005
S = 1.01; r^2 = 1.00

(a9) OM/OC=1.64; O/C=0.34; H/C=1.80; N/C=0.031
(b9) OM/OC=1.74; O/C=0.41; H/C=1.81; N/C=0.033
S = 0.93; r^2 = 0.95

(a10) OM/OC=1.61; O/C=0.31; H/C=1.98; N/C=0.025
(b10) OM/OC=1.74; O/C=0.41; H/C=1.92; N/C=0.027
S = 0.96; r^2 = 0.87

(a11) OM/OC=1.38; O/C=0.15; H/C=2.09; N/C=0.012
(b11) OM/OC=1.41; O/C=0.17; H/C=2.07; N/C=0.016
S = 1.02; r^2 = 1.00

(a12) OM/OC=1.57; O/C=0.28; H/C=1.85; N/C=0.038
(b12) OM/OC=1.59; O/C=0.29; H/C=1.86; N/C=0.040
S = 1.00; r^2 = 1.00

(a13) OM/OC=1.55; O/C=0.26; H/C=1.86; N/C=0.034
(b13) OM/OC=1.56; O/C=0.27; H/C=1.88; N/C=0.039
S = 0.98; r^2 = 0.99

% of the total signal
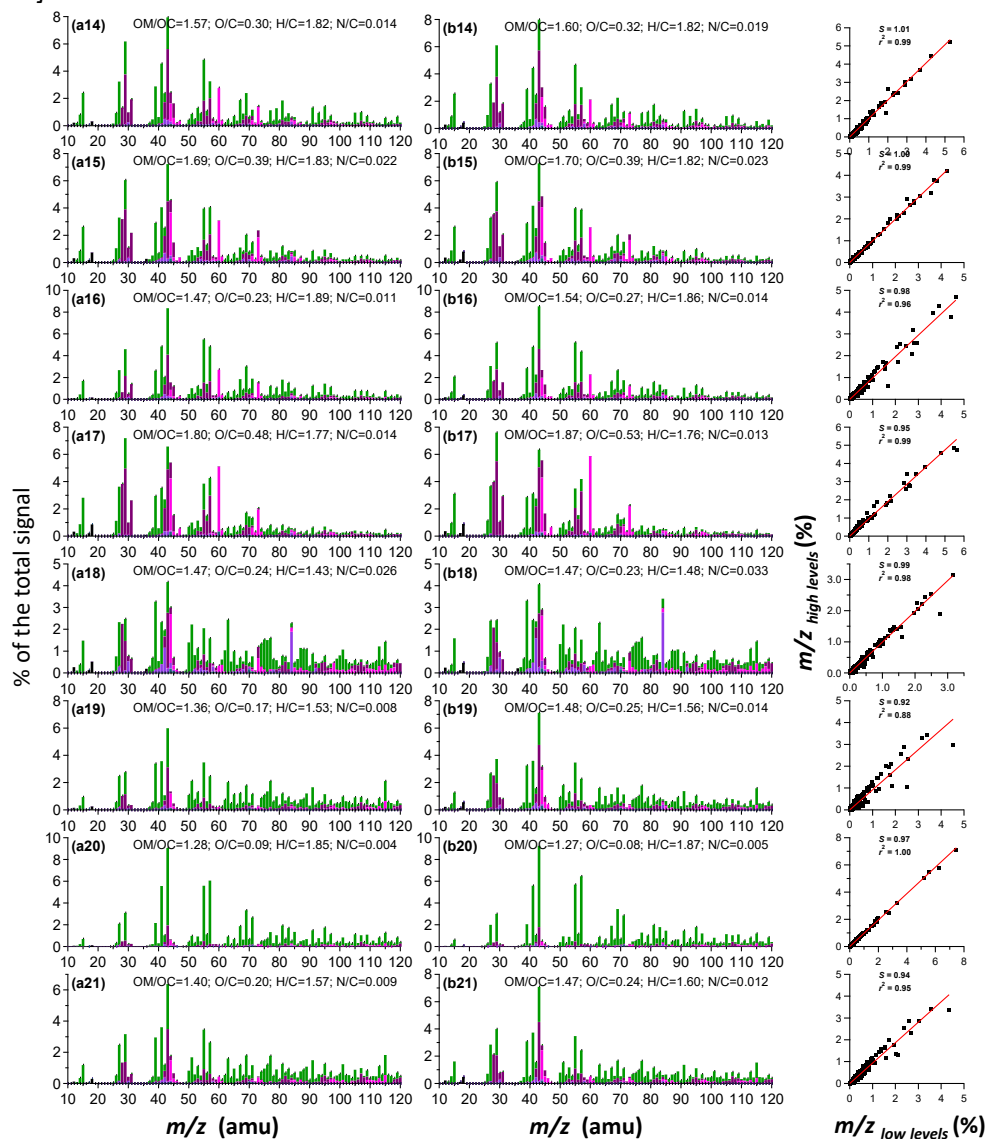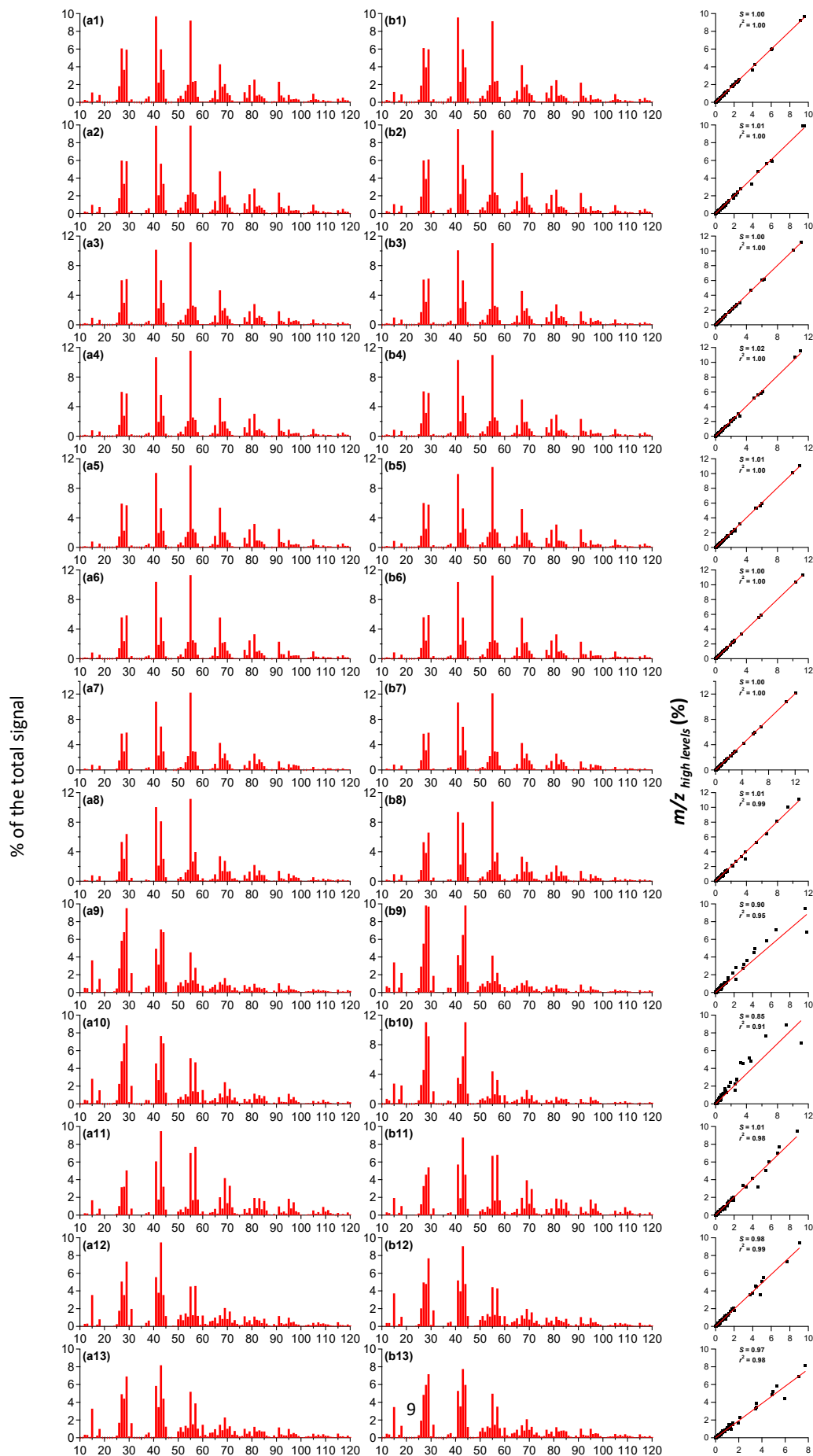
m/z $_{high\ levels}$ (%)

7

[continued]

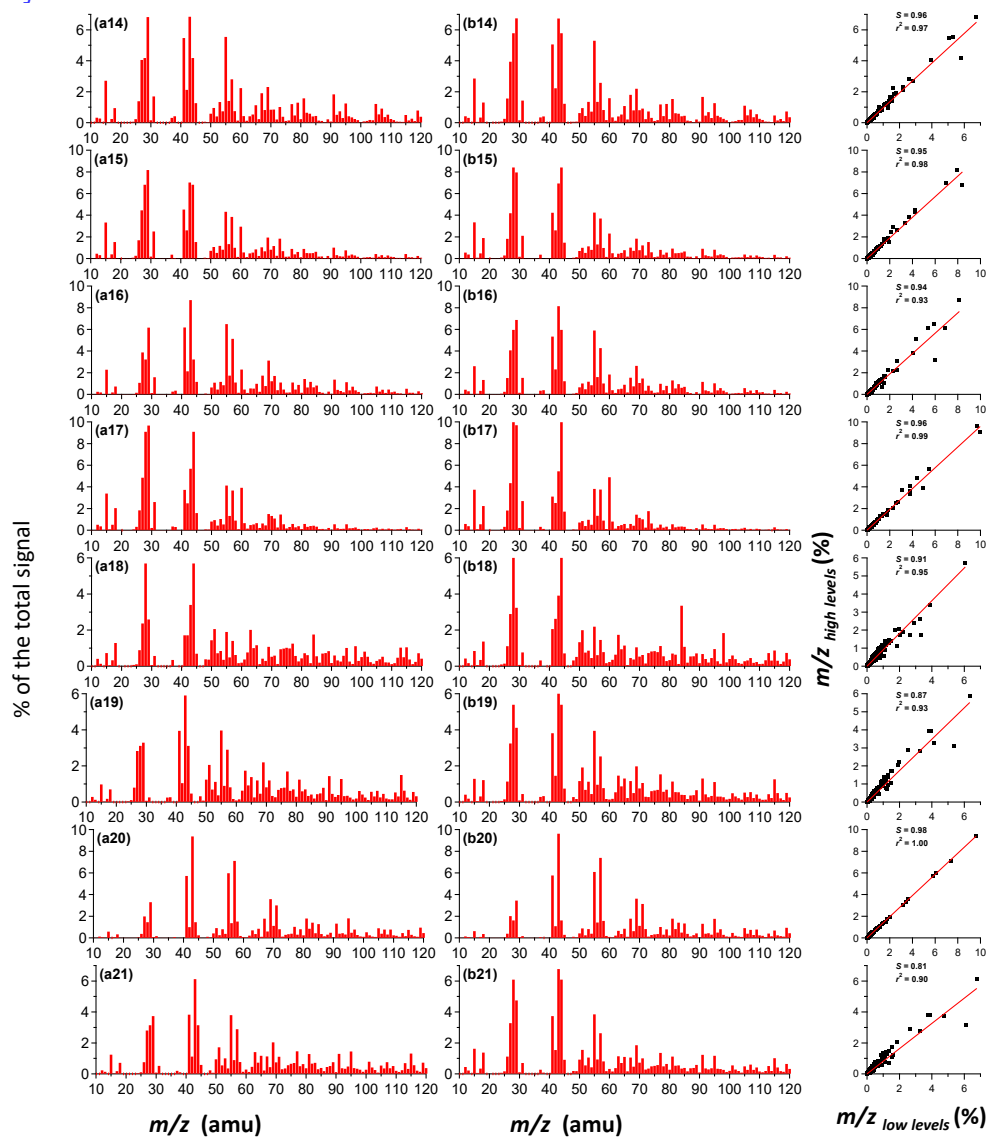Figure S1. The mass spectral profiles of OA measured by SV-AMS at (a) high and (b) low levels from (1) stir-fried garlic with corn oil, (2) stir-fried celery with corn oil, (3) peanut oil, (4) bean oil, (5) sunflower oil, (6) blend oil, (7) lard oil and (8) barbecue (9) wheat, (10) corn, (11) bean, (12) rape, (13) cotton, (14) birchen, (15) pine tree, (16) poplar, (17) Chinese oak, (18) flaming combustion of brown coal, (19) smoldering combustion of brown coal, (20) flaming combustion of bituminous coal and (21) smoldering combustion of bituminous coal. The comparison of mass spectrum for each experiment is shown. The detailed descriptions of cooking and burning fuels are presented in Table S1.

9

Figure S2. The mass spectral profiles of OA measured by CV-ACSM at (a) high and (b) low levels from (1) stir-fried garlic with corn oil, (2) stir-fried celery with corn oil, (3) peanut oil, (4) bean oil, (5) sunflower oil, (6) blend oil, (7) lard oil and (8) barbecue (9) wheat, (10) corn, (11) bean, (12) rape, (13) cotton, (14) birchen, (15) pine tree, (16) poplar, (17) Chinese oak, (18) flaming combustion of brown coal, (19) smoldering combustion of brown coal, (20) flaming combustion of bituminous coal and (21) smoldering combustion of bituminous coal. The comparison of mass spectrum for each experiment is shown. The detailed descriptions of cooking and burning fuels are presented in Table S2.

Table S1. A summary of f_{44}, f_{43}, f_{60} and OA concentration (μg m^{-3}) at high and low OA levels measured by SV-AMS in each experiment. The default RIE (1.4) and CE=1 were used.

Fuels	OA	f_{44}	f_{43}	f_{60}	OA	f_{44}	f_{43}	f_{60}
	High Conc.				Low Conc.			
CornOil1	503.9	0.027	0.078	0.006	382.9	0.029	0.077	0.006
CornOil2	507.7	0.029	0.074	0.006	382.6	0.030	0.073	0.006
Peanut	564.3	0.021	0.077	0.008	388.8	0.023	0.077	0.008
BeanOil	485.0	0.023	0.068	0.006	338.3	0.024	0.069	0.006
Sunflower	624.0	0.017	0.070	0.007	388.3	0.019	0.070	0.007
BlendOil	666.9	0.020	0.070	0.006	313.8	0.023	0.070	0.006
LardOil	221.4	0.029	0.082	0.008	162.2	0.030	0.082	0.007
BBQ	421.7	0.014	0.095	0.010	150.4	0.018	0.094	0.009
Wheat	862.7	0.027	0.077	0.017	79.4	0.041	0.077	0.015
Corn	548.2	0.031	0.102	0.032	151.0	0.047	0.084	0.023
Bean	849.2	0.016	0.101	0.008	364.0	0.021	0.099	0.007
Rape	642.1	0.021	0.093	0.017	241.5	0.025	0.092	0.017
Cotton	742.0	0.023	0.084	0.019	264.9	0.028	0.084	0.016
Birchen	338.4	0.025	0.079	0.028	150.4	0.031	0.080	0.021
Pine	361.0	0.047	0.072	0.031	173.8	0.050	0.073	0.026
Poplar	1369.6	0.016	0.084	0.027	185.6	0.028	0.085	0.023
Oak	513.5	0.055	0.066	0.051	201.5	0.056	0.063	0.059
BrCoalF	154.2	0.029	0.042	0.003	154.4	0.029	0.041	0.003
BrCoalS	269.8	0.014	0.060	0.002	103.1	0.034	0.071	0.003
BiCoalF	376.4	0.006	0.091	0.001	339.4	0.005	0.092	0.001
BiCoalS	275.8	0.018	0.064	0.004	120.6	0.029	0.071	0.005

Note: CornOil1= stir-fried garlic with corn oil; CornOil2= stir-fried celery with corn oil; Peanut= stir-fried celery with peanut oil; Sunflower= stir-fried celery with sunflower oil; BeanOil= stir-fried celery with bean oil; BlendOil= stir-fried celery with blend oil; LardOil= stir-fried celery with lard oil; BBQ= barbecue; Wheat= dry wheat stalk burning; Corn= dry corn stalk burning; Bean= dry bean stalk burning; Rape= dry rape stalk burning; Cotton= dry cotton stalk burning; Birchen= dry birchen burning; Pine= dry pine tree burning; Poplar= dry poplar burning; Oak= dry Chinese oak burning; BrCoalF= brown coal combustion under flaming conditions; BrCoalS= brown coal combustion under smoldering conditions; BiCoalF= bituminous coal combustion under flaming conditions; BiCoalS= bituminous coal combustion under smoldering conditions.

Table S2. A summary of f_{44}, f_{43}, f_{60} and OA concentration (µg m^{-3}) at high and low OA levels measured by CV-ACSM in each experiment. The default RIE (1.4) and CE=1 were used.

Fuels	OA	f_{44}	f_{43}	f_{60}	OA	f_{44}	f_{43}	f_{60}
	High Conc.				Low Conc.			
CornOil1	715.3	0.037	0.060	0.001	517.0	0.039	0.060	0.001
CornOil2	714.4	0.033	0.056	0.001	265.3	0.039	0.055	0.000
Peanut	799.2	0.030	0.060	0.001	676.5	0.031	0.060	0.001
BeanOil	613.9	0.028	0.056	0.001	286.7	0.032	0.055	0.001
Sunflower	1064.2	0.023	0.053	0.001	730.2	0.025	0.053	0.001
BlendOil	927.0	0.024	0.056	0.001	829.7	0.024	0.056	0.001
LardOil	518.7	0.029	0.069	0.001	366.6	0.031	0.068	0.001
BBQ	290.4	0.030	0.081	0.004	102.5	0.038	0.079	0.003
Wheat	294.8	0.068	0.071	0.008	83.3	0.098	0.065	0.006
Corn	523.5	0.068	0.077	0.016	119.8	0.110	0.064	0.012
Bean	893.0	0.032	0.095	0.004	279.7	0.046	0.088	0.004
Rape	683.8	0.035	0.095	0.012	172.8	0.048	0.090	0.011
Cotton	615.2	0.044	0.082	0.015	188.1	0.060	0.077	0.012
Birchen	558.3	0.042	0.068	0.022	206.8	0.058	0.067	0.016
Pine	402.8	0.068	0.070	0.029	107.1	0.084	0.069	0.023
Poplar	616.4	0.032	0.087	0.023	104.8	0.060	0.081	0.018
Oak	485.9	0.091	0.057	0.039	133.4	0.100	0.054	0.049
BrCoalF	121.6	0.057	0.034	0.002	82.1	0.061	0.039	0.002
BrCoalS	269.4	0.031	0.059	0.001	104.8	0.054	0.063	0.001
BiCoalF	334.9	0.015	0.094	0.001	241.4	0.016	0.096	0.001
BiCoalS	276.8	0.031	0.061	0.003	101.4	0.061	0.068	0.003

Note: CornOil1= stir-fried garlic with corn oil; CornOil2= stir-fried celery with corn oil; Peanut= stir-fried celery with peanut oil; Sunflower= stir-fried celery with sunflower oil; BeanOil= stir-fried celery with bean oil; BlendOil= stir-fried celery with blend oil; LardOil= stir-fried celery with lard oil; BBQ= barbecue; Wheat= dry wheat stalk burning; Corn= dry corn stalk burning; Bean= dry bean stalk burning; Rape= dry rape stalk burning; Cotton= dry cotton stalk burning; Birchen= dry birchen burning; Pine= dry pine tree burning; Poplar= dry poplar burning; Oak= dry Chinese oak burning; BrCoalF= brown coal combustion under flaming conditions; BrCoalS= brown coal combustion under smoldering conditions; BiCoalF= bituminous coal combustion under flaming conditions; BiCoalS= bituminous coal combustion under smoldering conditions.

Technical Remarks:

"/" in "m/z" should not be italized.

Changed

References

Faber, P., Drewnick, F., Veres, P. R., Williams, J., and Borrmann, S.: Anthropogenic sources of aerosol particles in a football stadium: Real-time characterization of emissions from cigarette smoking, cooking, hand flares, and color smoke bombs by high-resolution aerosol mass spectrometry, Atmos. Environ., 77, 1043-1051, 10.1016/j.atmosenv.2013.05.072, 2013.

Fang, Z., Deng, W., Zhang, Y. L., Ding, X., Tang, M. J., Liu, T. Y., Hu, Q. H., Zhu, M., Wang, Z. Y., Yang, W. Q., Huang, Z. H., Song, W., Bi, X. H., Chen, J. M., Sun, Y. L., George, C., and Wang, X. M.: Open

burning of rice, corn and wheat straws: primary emissions, photochemical aging, and secondary organic aerosol formation, Atmos. Chem. Phys., 17, 14821-14839, 10.5194/acp-17-14821-2017, 2017.

Jolleys, M. D., Coe, H., McFiggans, G., Taylor, J. W., O'Shea, S. J., Le Breton, M., Bauguitte, S. J. B., Moller, S., Di Carlo, P., Aruffo, E., Palmer, P. I., Lee, J. D., Percival, C. J., and Gallagher, M. W.: Properties and evolution of biomass burning organic aerosol from Canadian boreal forest fires, Atmos. Chem. Phys., 15, 3077-3095, 10.5194/acp-15-3077-2015, 2015.

Kaltsonoudis, C., Kostenidou, E., Louvaris, E., Psichoudaki, M., Tsiligiannis, E., Florou, K., Liangou, A., and Pandis, S. N.: Characterization of fresh and aged organic aerosol emissions from meat charbroiling, Atmos. Chem. Phys., 17, 7143-7155, 10.5194/acp-17-7143-2017, 2017.

Li, Y. C., Qiu, J. Q., Shu, M., Ho, S. S. H., Cao, J. J., Wang, G. H., Wang, X. X., and Zhao, X. Q.: Characteristics of polycyclic aromatic hydrocarbons in PM2.5 emitted from different cooking activities in China, Environ. Sci. Pollut. Res., 25, 4750-4760, 10.1007/s11356-017-0603-0, 2018.

Liu, T., Wang, Z., Wang, X., and Chan, C. K.: Primary and secondary organic aerosol from heated cooking oil emissions, Atmos. Chem. Phys., 18, 11363-11374, 10.5194/acp-18-11363-2018, 2018.

Liu, T. Y., Li, Z. J., Chan, M. N., and Chan, C. K.: Formation of secondary organic aerosols from gas-phase emissions of heated cooking oils, Atmos. Chem. Phys., 17, 7333-7344, 10.5194/acp-17-7333-2017, 2017.

McLafferty, F. W., and Turecek, F.: Interpretation of Mass Spectra, University Science Books, Mill Valley, California, 1993.

Qiu, Y., Xie, Q., Wang, J., Xu, W., Li, L., Wang, Q., Zhao, J., Chen, Y., Chen, Y., Wu, Y., Du, W., Zhou, W., Lee, J., Zhao, C., Ge, X., Fu, P., Wang, Z., Worsnop, D. R., and Sun, Y.: Vertical Characterization and Source Apportionment of Water-Soluble Organic Aerosol with High-resolution Aerosol Mass Spectrometry in Beijing, China, ACS Earth and Space Chemistry, 3, 273-284, 10.1021/acsearthspacechem.8b00155, 2019.

Reyes-Villegas, E., Bannan, T., Le Breton, M., Mehra, A., Priestley, M., Percival, C., Coe, H., and Allan, J. D.: Online Chemical Characterization of Food-Cooking Organic Aerosols: Implications for Source Apportionment, Environ. Sci. Technol., 52, 5308-5318, 10.1021/acs.est.7b06278, 2018.

Sciare, J., d'Argouges, O., Sarda-Estève, R., Gaimoz, C., Dolgorouky, C., Bonnaire, N., Favez, O., Bonsang, B., and Gros, V.: Large contribution of water-insoluble secondary organic aerosols in the region of Paris (France) during wintertime, J. Geophys. Res., doi:10.1029/2011JD015756, 2011.

Sun, Y., He, Y., Kuang, Y., Xu, W., Song, S., Ma, N., Tao, J., Cheng, P., Wu, C., Su, H., Cheng, Y., Xie, C., Chen, C., Lei, L., Qiu, Y., Fu, P., Croteau, P., and Worsnop, D. R.: Chemical Differences Between PM1 and PM2.5 in Highly Polluted Environment and Implications in Air Pollution Studies, Geophys. Res. Lett., 47, e2019GL086288, 10.1029/2019gl086288, 2020.

Timonen, H., Saarikoski, S., Tolonen-Kivimäki, O., Aurela, M., Saarnio, K., Petäjä, T., Aalto, P., Kulmala, M., Pakkanen, T., and Hillamo, R.: Size distributions, sources and source areas of water-soluble organic carbon in urban background air, 2008.

Xu, L., Guo, H., Weber, R. J., and Ng, N. L.: Chemical Characterization of Water-Soluble Organic Aerosol in Contrasting Rural and Urban Environments in the Southeastern United States, Environ. Sci. Technol., 51, 78-88, 10.1021/acs.est.6b05002, 2017.

Zheng, Y., Cheng, X., Liao, K., Li, Y., Li, Y., Huang, R. J., Hu, W., Liu, Y., Zhu, T., Chen, S., Zeng, L., Worsnop, D. R., and Chen, Q.: Characterization of Anthropogenic Organic Aerosols by TOF-ACSM with the New Capture Vaporizer, Atmos. Meas. Tech. Discuss., 2020, 1-24, 10.5194/amt-2019-449, 2020.

Mass ~~Spectral Characterization~~spectral characterization of ~~Primary Emissions~~primary emissions and ~~Implications~~implications in ~~Source Apportionment~~source apportionment of ~~Organic Aerosol~~organic aerosol

Weiqi Xu[1,#], Yao He[1,2,#], Yanmei Qiu[1,2], Chun Chen[1,2], Conghui Xie[1,2], Lu Lei[1,2], Zhijie Li[1,2], Jiaxing Sun[1,2], Junyao Li[1,2], Pingqing Fu[3], Zifa Wang[1,2], Douglas R. Worsnop[4], and Yele Sun[1,2,5,*]

[1]State Key Laboratory of Atmospheric Boundary Layer Physics and Atmospheric Chemistry, Institute of Atmospheric Physics, Chinese Academy of Sciences, Beijing 100029, China
[2]University of Chinese Academy of Sciences, Beijing 100049, China
[3]Institute of Surface-Earth System Science, Tianjin University, Tianjin 300072, China
[4]Aerodyne Research Inc., Billerica, Massachusetts 01821, USA
[5]~~Center for Excellence in Regional Atmospheric Environment, Institute of Urban Environment, Chinese Academy of Sciences, Xiamen 361021, China~~[5]Collaborative Innovation Center on Forecast and Evaluation of Meteorological Disasters, Nanjing University of Information Science & Technology, Nanjing 210044, China

#These authors contributed equally

Correspondence: Yele Sun (sunyele@mail.iap.ac.cn)

Abstract. Source apportionment of organic aerosol (OA) from aerosol mass spectrometer (AMS) or aerosol chemical speciation monitor (ACSM) measurements relies largely upon mass spectral profiles from different source emissions. However, the changes in mass spectra of primary emissions from AMS/ACSM with the newly developed capture vaporizer (CV) are poorly understood. Here we conducted 21 cooking, crop straw, wood, and coal burning experiments to characterize the mass spectral features of OA and water-soluble OA (WSOA) using SV-AMS and CV-ACSM. Our results show overall similar spectral characteristics between SV-AMS and CV-ACSM for different primary emissions despite additional thermal decomposition in CV, and the previous spectral features for diagnostic of primary OA factors are generally well retained. However, the mass spectral differences between OA and WSOA can be substantial for both SV-AMS and CV-ACSM. The changes in f_{55} (fraction of m/z 55 in OA) vs. f_{57}, f_{44} vs. f_{60}, f_{44} vs. f_{43} in CV-ACSM are also observed, yet the evolving trends are similar to those of SV-AMS. By applying the source spectral profiles to a winter CV-ACSM study at a highly polluted rural site in North China Plain, the source apportionment of primary OA was much improved highlighting the two most important primary sources of biomass burning and coal combustion (32% and 21%). Considering the rapidly increasing deployments of CV-ACSM and WSOA studies worldwide, the mass spectral characterization has significant implications by providing essential constrains for more accurate source apportionment, and making better strategies for air pollution control in regions with diverse primary emissions.————

1 Introduction

Organic aerosol (OA) is ubiquitous in the atmosphere and often contributes a large fraction of aerosol particles. Currently, Aerodyne aerosol mass spectrometer (AMS) is one of the most widely used instruments for real-time measurements of OA (Canagaratna et al., 2007~~;Li et al., 2017)~~;Li et al., 2017). OA can be further separated into primary OA (POA) and secondary

5   OA (SOA) factors by using receptor models, e.g., positive matrix factorization (PMF) and multilinear engine (ME-2) ~~(Paatero, 1999;Paatero and Tapper, 1994)~~(Paatero, 1999;Paatero and Tapper, 1994). The determination of OA factors relies strongly upon the comparisons with collocated measurements and also the mass spectral profiles of primary emissions. However, in the absence of collocated measurements, the spectral features become the most important constrain for selection of PMF factors. As a result, the mass spectra of primary emissions have been extensively characterized with quadrupole- and high-resolution

10   time-of-flight AMS, including traffic exhaust (Canagaratna et al., 2004;Collier et al., 2015), biomass burning ~~(Schneider et al., 2006;~~(Schneider et al., 2006;Alfarra et al., 2007) and cooking emissions ~~(Mohr et al., 2009;He et al., 2010;~~(Mohr et al., 2009;He et al., 2010;Allan et al., 2010~~;Robinson et al., 2018)~~;Robinson et al., 2018), and the spectral characteristics, e.g., hydrocarbon ion series $C_nH_{2n-1}^+$ and $C_nH_{2n+1}^+$ for traffic emissions, f_{60} (fraction of m/z 60 in OA) for biomass burning, and high f_{55}/f_{57} for cooking OA, are widely used as diagnostics for the presence of OA factors. However, coal combustion emissions,

15   one of the most important primary sources in north China in winter, are rarely characterized ~~(Lin et al., 2017)~~(Lin et al., 2017). ~~Owning~~Owing to the relatively similar spectra between coal combustion OA (CCOA) and traffic-related hydrocarbon-like OA (HOA), and the decreases in coal combustion emissions in Beijing in recent years, it becomes more challenging to separate these two fossil-fuel-related factors ~~(Sun et al., 2016a;Xu et al., 2019)~~(Sun et al., 2016a;Xu et al., 2019), particularly for unit mass resolution spectra measured by aerosol chemical speciation monitor (ACSM). Therefore, it is of great importance to

20   characterize the spectral features of CCOA for a better quantification of coal combustion emissions.

Although AMS/ACSM is capable of measuring OA in real-time, the uncertainties in quantification can be up to 38% (Bahreini et al., 2009) mainly due to the influence of collection efficiency (CE) caused by particle bouncing from the vaporizer ~~(Huffman et al., 2005;Matthew et al., 2008)~~(Huffman et al., 2005;Matthew et al., 2008). While the parameterization of CE as a function of particle phase, acidity, and the fraction of ammonium nitrate ~~(Middlebrook et al., 2012)~~(Middlebrook et al., 2012) has

25   improved the AMS/ACSM quantification, the applications for the $PM_{2.5}$ lens and particles larger than 1 μm remain unknown. As a result, a new capture vaporizer (CV) with an enclosed cavity was developed ~~(Xu et al., 2017b)~~(Xu et al., 2017b). Field measurements showed that the CE of CV-AMS was fairly robust at ~1 ~~(Hu et al., 2017)~~(Hu et al., 2017). However, the OA mass spectra can have significant changes in CV by shifting towards smaller fragments compared to standard vaporizer (SV) due to additional thermal decomposition ~~(Hu et al., 2018a;Hu et al., 2018b)~~(Hu et al., 2018a;Hu et al., 2018b). To our

30   knowledge, the mass spectral differences between CV and SV, and the mass spectral features of primary emissions in CV-AMS/ACSM have not been well understood yet. Hence, it is critically important to re-characterize the mass spectra of primary

emissions in CV, and to provide essential constrains for OA source apportionment from the rapidly increasing CV-ACSM measurements worldwide.

In recent years, water-soluble OA (WSOA) which plays an important role in affecting aerosol hygroscopicity and cloud condensation nuclei formation, has attracted an increasing attention(Bozzetti et al., 2017;~~Xu et al., 2017a~~Xu et al., 2017a;~~Qiu et al., 2019~~Qiu et al., 2019;~~Ye et al., 2017~~Ye et al., 2017). Due to the challenges in real-time on-line measurements of WSOA, most previous studies focus on offline analysis of WSOA using SV-AMS. The results showed that oxygenated OA (OOA) and biomass burning OA (BBOA) are generally more water-soluble than other primary sources emissions, e.g., traffic and cooking (~~Mayol-Bracero et al., 2002~~(Mayol-Bracero et al., 2002;Daellenbach et al., 2016). Because of the different water-solubility of OA factors, the mass spectra of WSOA can be substantially different from the total OA which increases the difficulties in separation of the WSOA factors in source apportionment of WSOA. Although several studies tried to use ME-2 for a better source apportionment of less water-soluble components, e.g., HOA and cooking OA (COA), by using the ambient resolved spectra as constraints (Bozzetti et al., 2017;Daellenbach et al., 2016), it could introduce additional uncertainties ~~if~~when water-soluble HOA and COA were different from the constrained spectra. Unfortunately, mass spectral characterization of WSOA from different primary emissions using SV-AMS and CV-ACSM is extremely limited. Thus, there is an urgent need for characterization of the mass spectra of WSOA from different primary emissions, which has a great potential to improve the future source apportionment of WSOA.

In this work, we conducted 21 cooking and burning experiments to characterize the mass spectral features of OA and water-soluble OA from cooking emissions, crop straw burning, wood burning and coal combustion using SV-AMS and CV-ACSM. The mass spectra of OA and WSOA from CV-ACSM are compared with those of SV-AMS, and the changes in specific marker m/z's for different primary sources are elucidated. In particular, we demonstrate the importance of applying mass spectra of primary emissions to receptor models for a better source apportionment of OA in a highly polluted environment with complex primary emissions.

2 Experimental methods

2.1 Experimental set-up

21 experiments were conducted including 7 cooking with different oils (stir-fried garlic with corn oil, stir-fried celery with corn oil, peanut oil, bean oil, sunflower oil, blend oil, and lard oil), one barbecue, 6 crop straw burning (dry wheat, corn, bean, rape, and cotton) and 4 wood burning (dry birchen, pine tree, poplar, and Chinese oak) under smoldering-dominated conditions, and 4 coal combustion (brown and bituminous coal) under both flaming and smoldering conditions in June 2019. The average

(±1σ) temperature and relative humidity during the experiments were 24.6 (±3.4) °C and 59.5 (±23.1) %. All fuels were burned in a common residential stove outside a 50 m³ tent, and aerosol particles were then emitted into the tent through a chimney (Fig. S1). After approximately 5 min, a high volume sampler (TISCH) was first used to collect $PM_{2.5}$ samples for 10 min, then a HR-AMS equipped with an SV and PM_1 lens (SV-AMS hereafter) and a ToF-ACSM equipped with a CV and $PM_{2.5}$ lens (CV-ACSM hereafter) were operated in parallel to measure organic aerosol particles for approximately 15 min. Because the real-time measurements of CO_2 were not available, a HEPA filter was placed in the front of the sampling line before and after the SV-AMS and CV-ACSM measurements to correct the influence of gaseous CO_2 on the total m/z 44. After the burning experiment, the room was ventilated completely until the mass concentrations of aerosol particles were close to the ambient values that were measured by the other CV-ACSM nearby. Note that the average mass loadings of OA during the burning experiments are nearly 2 order of magnitude of that in ambient air, indicating the negligible influences of background OA to our experiments.

Cooking experiments were conducted inside the tent by simulating the real Chinese cooking styles with different oils. To avoid the influences from burning of the fuel, an induction cooker was used in this study. In comparison, the barbecue experiment was performed using mutton shashlik and anthracite as ingredient and fuel, respectively, which are the most popular barbecue styles in restaurants. Burning anthracite alone was found to emit significantly lower mass loadings of aerosol particles than those emitted from barbecue.

The average mass loadings of OA during the burning and cooking experiments are nearly 2 order of magnitude of that in ambient air, indicating the negligible influences of background OA to our experiments. As shown in Table S1, the mass concentrations of OA measured by SV-AMS ranged from ~80 μg m⁻³ to ~1370 μg m⁻³ for different burning experiments by using a relative ionization efficiency of 1.4 and a collection efficiency of 1. Considering that the mass spectra of OA can have changes across different mass loadings due to the partitioning of semi-volatile organic compounds (Donahue et al., 2006; Shilling et al., 2009), we further checked the spectral differences between high and low mass loadings for SV-AMS and CV-ACSM (Tables S1 and S2, respectively). As indicated in Figures S1 and S2, the mass spectra of OA, and f_{44}, f_{43}, and f_{60} from cooking and flaming combustion of coal are remarkably similar under low and high mass loadings, indicating that the mass spectra are relatively stable upon dilution or evaporation, and thus can be well used as constraints in source apportionment analysis. Although the mass spectra of OA for the rest burning, i.e., biomass burning, wood burning, and smoldering combustion of coal are also highly similar between low and high mass loadings, the ubiquitous increases in f_{44} and corresponding decreases in f_{60} were observed from high to low mass loadings. For instance, f_{44} in SV-AMS was increased by 0.4 – 2% as the mass loading decreased by a factor of ~3, and f_{60} showed a corresponding decrease by 0.1 – 0.9%. Similarly, f_{44} in CV-ACSM was increased by 0.9 – 4.2% associated with a decrease in f_{60} by 0.1 – 0.6% as OA mass loadings were decreased by a factor of ~3 – 4. Such results are consistent with previous studies that biomass burning OA can be rapidly aged

4

in the atmosphere which is characterized by increases in f_{44} and decreases in f_{60} (Cubison et al., 2011; Morgan et al., 2020). Therefore, source apportionment of OA using the source spectra from biomass burning, wood burning and smoldering combustion of coal need to consider the mass loading effects and increase the variability uncertainties in f_{44} and f_{60}.

2.2 Chemical and data analysis

The PIKA 1.57 and Tofware v2.5.13 were used for determination of mass concentrations and mass spectra of OA measured by SV-AMS and CV-ACSM, respectively. The elemental ratios of OA measured by SV-AMS including hydrogen-to-carbon (H/C), oxygen-to-carbon(O/C), nitrogen-to-carbon (N/C) and organic mass-to-organic carbon (OM/OC) ratios in this study were calculated using the Improved-Ambient (I-A) method (Canagaratna et al., 2015). The offline analysis of WSOA with SV-AMS and CV-ACSM is similar to that reported in our previous study (Qiu et al., 2019)(Qiu et al., 2019). Briefly, 2 or 3 punches of filter samples were sonicated in 25 mL deionized water, and then filtered with 0.45 μm syringe filters (Anpel, PVDF). An aliquot of the solution was atomized using pure argon, dried by the nafion dryer, and then simultaneously measured by SV-AMS and CV-ACSM. Different from WSOA in ambient aerosol (Qiu et al., 2019)(Qiu et al., 2019), the ratio of CO^+/CO_2^+ varied largely among different burning experiments, for example, 0.78 – 1.40 for cooking, 2.07 – 2.53 for crop straw burning, 1.50 – 2.45 for wood burning, and 1.50- 1.85 for coal combustion (Fig. S22). For a better comparison with OA measured by SV-AMS, CO^+ was scaled to be equal to CO_2^+ for all WSOA samples. We found that the O/C ratios calculated with $CO^+ = CO_2^+$ and the fitted values have differences by 0.6 – 11.6%. In addition, organic carbon (OC), elemental carbon (EC), and water-soluble OC (WSOC) in PM$_{2.5}$ samples were analyzed by a Sunset OC/EC analyzer (Sunset Laboratory Inc., Model-4) and a total organic carbon (TOC) analyzer (Shimadzu, TOC-L), respectively. A more detailed description of carbonaceous aerosol analysis is given elsewhere (Li et al., 2018)(Li et al., 2018).

3 Results and discussion

3.1 Cooking emissions

The mass spectral profiles of 8 cooking OA are shown in Figs. 13-4 and S3. All COA spectral profiles measured by SV-AMS and CV-ACSM are highly similar (R^2>0.89, Fig. 25), and also resemble those previously resolved in ambient air during all seasons in Beijing (Fig. S4).S4) despite the COA concentrations can have a difference of an order of magnitude. We also noticed slightly higher O/C (f_{44}) for COA under lower mass loadings, which were likely due to partitioning of more semi-volatile organics on particles during periods with higher mass loadings (Reyes-Villegas et al., 2018a). These results suggest fairly robust COA spectra for different cooking oils. One explanation is the relatively similar ingredients of cooking oils that are generally dominated by fatty acids and carbonyls (Schauer et al., 2002)(Schauer et al., 2002). Consistent with previous

5

studies ~~(Sun et al., 2011;Mohr et al., 2012)~~(Sun et al., 2011;Mohr et al., 2012), the source spectra of COA from SV-AMS are characterized by high f_{55}/f_{57} (fraction of m/z 55 and 57 in OA, respectively) ratios (2.0–2.7), and low O/C ratios (0.15 – 0.18). These results indicate that the COA source spectra can be used as good constraints for a better source apportionment of COA. We also observed considerable N-containing ions in COA spectra, and the average N/C ratios ranged from 0.005 to 0.033. Such high N/C ratios suggest that cooking emissions can be a significant source of organic nitrogen (ON) in ambient air, in agreement with our previous study showing two ON peaks during mealtimes ~~(Xu et al., 2017d)~~(Xu et al., 2017d), and also the ubiquitous identification of nitrogen-containing compounds from cooking emissions ~~(Reyes Villegas et al., 2018a)~~(Reyes-Villegas et al., 2018a). Note that the N/C ratio of ambient COA identified by PMF in Beijing (0.002-0.015) ~~(Sun et al., 2016a;Xu et al., 2017c;Xu et al., 2019)~~(Sun et al., 2016a;Xu et al., 2017c;Xu et al., 2019) is generally lower than those from cooking emissions (Fig. S5). One reason is due to the challenges in separation and quantification of N-containing ions in ambient OA, particularly for the low mass resolution V-mode measurements. We also noticed pronounced m/z 60 (f_{60}=0.57-0.96%) and m/z 73 (f_{73}=0.59-1.1%) in COA source spectra, which are generally used as biomass burning tracers (Cubison et al., 2011). ~~However, the ratios of f_{60}/f_{73} in COA from SV AMS are fairly constant (~1, Fig. 3), which are approximately twice lower than those observed in biomass burning OA (~2, Fig. 3).~~Because an induction cooker was used in this study, the signals of f_{60} and f_{73} would be completely from cooking oils. Previous studies also observed such signals from laboratory-generated cooking emissions, for example, palm oil COA (Liu et al., 2018;Liu et al., 2017), fresh COA (Kaltsonoudis et al., 2017), heating of frying oil and deep-frying (Faber et al., 2013). Although the chemical ionization mass spectrometer was able to detect high concentrations of levoglucosan in cooking emissions (Reyes-Villegas et al., 2018a), the ratios of f_{60}/f_{73} in COA from SV-AMS are fairly constant (~1, Fig. 6), which are approximately twice lower than those observed in biomass burning OA (~2, Fig. 6). These results highlight the contributions of other cooking-related oxygenated compounds to m/z 60 and m/z 73.

As shown in Figs. ~~1~~3 and S6, all COA spectra of CV-ACSM are fairly stable and overall similar to those of SV-AMS (R^2> 0.86). ~~Although previous studies~~ Due to additional thermal decomposition in CV, the COA source spectra in CV showed slightly higher f_{44} (2.4–3.7%) than that of SV-AMS (1.8–2.9%)~~(Hu et al., 2018a)~~(Hu et al., 2018a) ~~showed that OA spectra tend to shift towards small m/z's due to additional thermal decomposition in CV, the COA source spectra are found to be fairly stable in CV with slightly higher f_{44} (2.4–3.7%) than that of SV-AMS (1.8–2.9%).~~. The major COA spectral differences between CV-ACSM and SV-AMS are the changes in $C_nH_{2n-1}^+/C_nH_{2n+1}^+$ ratios, e.g., m/z 41/43, m/z 55/57, and m/z 67/69. For example, the m/z 55/57 ratios ranged from 2.8 to 5.4 in CV-ACSM, ~~which are approximately twice higher than those in SV AMS (2.0 – 2.7, Fig. 3,~~ which were consistent with those of cooking exhaust near a kitchen ventilator (4.05) measured by another similar CV-ACSM (Zheng et al., 2020), yet the ratios were approximately twice higher than those in SV-AMS (2.0 – 2.7, Fig. 6). Similarly, the ratios of m/z 41/43 and m/z 67/69 in CV-ACSM (1.2 – 1.9 and 1.2 – 2.6, respectively) are also much higher than those in SV-AMS. In addition, we found that the prominent m/z 60 and 73 signals in CV-ACSM were much smaller than those in SV-AMS, likely due to additional thermal decomposition in CV.

The mass spectra of water-soluble COA (WSCOA) are much different from those of total COA for both SV-AMS and CV-ACSM in terms of elemental composition and f_{44}. As indicated in Figs. ~~1~~4 and S3, the O/C ratios of WSCOA range from 0.33 to 0.45, which are much higher than 0.15-0.18 of COA, suggesting that WSCOA contains more oxygenated organic compounds. This is consistent with the much higher $C_xH_yO^+$ and $C_xH_yO_z^+$ families (23.4 – 34.5% and 10.0 – 12.5%, respectively) in WSCOA than COA (14.8 – 18.0% and 6.9 – 7.9%, respectively). Similarly, the f_{44} of WSCOA is higher than that in COA by more than a factor of 2. We also noticed much higher N/C ratios in WSCOA than COA, indicating enriched nitrogen-containing organic compounds in water-soluble COA. Despite the differences above, the mass spectral features of COA, i.e., high m/z 55 and 57, and m/z 55/57 ratio are well retained in WSCOA from animal oil for both SV-AMS and CV-ACSM (Fig. ~~1~~4), while there are more changes in WSCOA from vegetable oil with much reduced f_{55} and f_{57}. One reason is due to the different water solubility of COA between vegetable and animal oils. Our carbon analysis showed that COA from vegetable oil has higher water-solubility compared to that from animal oil as indicated by the higher WSOC/OC ratios (~30% vs. 17%). As a result, the O/C ratio and f_{44} in WSOA from vegetable oil are correspondingly higher than those from animal oil. By comparing with the source spectra of WSCOA, we found that the previously resolved ambient WSCOA in urban Beijing (O/C = 0.38 and WSCOA/OA = 19%) ~~(Qiu et al., 2019)~~(Qiu et al., 2019) tends to be a mixture from cooking both vegetable and animal oils.

3.2 Crop straw burning

The mass spectral profiles of biomass burning have been relatively well characterized by SV-AMS in previous studies ~~(Weimer et al., 2008;Lee et al., 2010;Schneider et al., 2006;~~(Weimer et al., 2008;Lee et al., 2010;Schneider et al., 2006;Alfarra et al., 2007), and m/z 60 (mainly $C_2H_4O_2^+$) and 73 (mainly $C_3H_5O_2^+$) from fragmentation of anhydrosugars (e.g., levoglucosan~~,~~) are widely used as biomass burning markers in ambient studies. We found that f_{60} measured by SV-AMS varied largely among different crop straw fuels ranging from 0.8% to 2.6% (Figs. ~~1~~3 and S3) which is generally close to the values reported in previous studies ~~(Sun et al., 2016b;Gilardoni et al., 2016)~~(Sun et al., 2016b;Gilardoni et al., 2016), but much higher than that from open straw burning (f_{60} = 0.3%-0.6%) ~~(Fang et al., 2017)~~(Fang et al., 2017). One explanation is that f_{60} depends on biomass fuels, burning conditions (e.g., flaming or smoldering), and also chemical aging ~~(Hennigan et al., 2011;Schneider et al., 2006~~(Hennigan et al., 2011;Schneider et al., 2006;Collier et al., 2016). In addition, we also observed relatively high fractions of $C_xH_yN_z^+$ in BBOA (4.2% - 10.2%) and high N/C ratios (0.014-0.039), consistent with the observations of abundant nitrogen-containing organic compounds, e.g., N-heterocyclic alkaloid compounds, amines and nitrated phenols from biomass burning ~~(Reyes-Villegas et al., 2018b~~(Reyes-Villegas et al., 2018b;Bottenus et al., 2018;~~Wang et al., 2017;Laskin et al., 2009~~Wang et al., 2017;Laskin et al., 2009;Desyaterik et al., 2013). Compared with SV-AMS, the BBOA spectra of CV-ACSM are overall similar (R^2 = 0.93 – 0.96, Fig. S6) except the burning of wheat and corn stalk (R^2 = 0.80). As expected, f_{60} in CV-ACSM is lower than that in SV-AMS (1.0% vs. 1.7%), while f_{44} is correspondingly higher (5.9% vs. 2.7%) due to strong thermal decomposition in CV. Although the f_{60} signal is low, it still can be used as a biomass burning marker for CV-

AMS/ACSM ~~(Hu et al., 2018a)~~(Hu et al., 2018a). It should be noted that the f_{44} of crop straw burning measured by CV in this study is lower than that identified in ambient aerosol by the ToF-ACSM in Gucheng ~~(He et al. in preparation),~~. likely indicating that ambient BBOA has been photochemically aged to some extent.

The mass spectra of water-soluble BBOA (WSBBOA) resemble those of BBOA for both SV-AMS and CV-ACSM (Figs. ~~1 and S3). One reason is due to the high solubility of BBOA with WSOC accounting for ~ 40 – 70% of OC. However, we also found that~~4 and S3). One reason is due to the high solubility of BBOA of which ~40 – 70% of carbon was found to be water-soluble. This is consistent with the observation from a combustion chamber experiment (65%) (Zheng et al., 2020). It should be noted that the f_{60} of WSBBOA measured by CV-ACSM in this study is higher than that reported in Zheng et al. (2020) likely due to the differences in combustion system and ACSM detectors. WSBBOA presents generally higher f_{60} and f_{44} than the total BBOA for SV-AMS (2.4% vs. 1.7%, and 4.1% vs. 2.7% respectively), and CV-ACSM (1.6 vs. 1.0%, and 8.7 vs. 5.9% respectively). As shown in Fig. S7, the slope of f_{44} is less than 1 for both SV-AMS and CV-ACSM, and all data points are located in the right-bottom corner, in agreement with the higher O/C ratios of WSOA than OA. In fact, the O/C ratios of WSBBOA is approximately 50% higher than those of BBOA although they are still lower than that (O/C = 0.59) identified in winter in urban Beijing ~~(Qiu et al., 2019)~~(Qiu et al., 2019). These results further suggest that WSOA contains more oxygenated organic compounds with higher oxidation degrees.

3.3 Wood burning

Crop straw burning contributes dominantly to BBOA in China during both harvest season and winter (Chen et al., 2017;~~Sun et al., 2016b~~Sun et al., 2016b), while wood burning is more important for domestic heating in European countries ~~(Mohr et al., 2011~~(Mohr et al., 2011;Alfarra et al., 2007). Here we found that the mass spectra of BBOA and wood burning OA (WBOA) show relatively similar features (Fig. ~~1~~3), which are both characterized by the prominent signals of m/z 60 and m/z 73. The f_{60}/f_{73} varies from 1 to 2 for WBOA and BBOA, which is larger than that in cooking emissions (f_{60}/f_{73} =~1) and CCOA (f_{60}/f_{73} < 1, Fig. ~~3~~6). Compared to crop straw burning, WBOA of SV-AMS generally shows much higher f_{60} (2.5 –5.7% vs. 0.8 – 2.6%) and f_{73} (1.3-2.3 vs. 0.6 – 1.4%), and higher oxidation degree with higher f_{44} (1.7-5.5% vs. 1.8-3.4%) and O/C (0.23-0.51 vs. 0.16 – 0.38). These results suggest that wood burning appears to produce more anhydrosugar compounds. Consistent with BBOA, WBOA of CV-ACSM shows much higher f_{44}, and slightly lower f_{60} than those of SV-AMS (Figs. ~~1~~3 and S3). However, considering the spectral similarities between BBOA and WBOA, it would be very challenging to separate the two different biomass burning OA based only on AMS or ACSM measurements.

The mass spectra of WBOA of CV-ACSM show highly similar characteristics to those of SV-AMS (R^2=0.88-0.94) although f_{60} is slightly lower and f_{44} is comparably higher. Similar to BBOA, the water-soluble WBOA is also characterized by prominent

peaks of m/z 60 and m/z 73 (Figs. ~~1~~3 and S3), and enriched in oxygenated and nitrogen-containing organic compounds (O/C = 0.36 – 0.54 and N/C = 0.016-0.076). In fact, a large fraction of OC from wood burning was found to be water-soluble (32 – 40%). The f_{44} vs. f_{60} plot has been widely used in both field and laboratory studies to characterize the aging of biomass burning OA (Cubison et al., 2011;~~Hennigan et al., 2011~~Hennigan et al., 2011). Photochemical aging of BBOA can be rapid under typical ambient OH levels, e.g., 1×10^6 molecules cm^{-3} ~~(Hennigan et al., 2010)~~(Hennigan et al., 2010), and BBOA evolves quickly from the right-bottom to left-top region in f_{44} vs. f_{60}, which is characterized by an increase in f_{44} and a corresponding decrease in f_{60}. Although f_{60} and f_{44} of CV-ACSM and water-soluble BBOA/WBOA have differences compared with those measured by SV-AMS, the evolving trends in f_{44} vs. f_{60} are similar (Fig. ~~3~~6). These results suggest that f_{44} vs. f_{60} can also be used as a good diagnostic for chemical aging of biomass burning aerosol that are measured by the CV-AMS/ACSM. It should be noted that some previous studies also found large differences in f_{60} between SV-AMS and CV-AMS. ~~For example, Hu et al. (2018a)~~For example, Hu et al. (2018a) found that the f_{60} of OA from CV-AMS was lower than that from SV-AMS by a factor of 5 during a period with significant BB impacts, yet the correlation was high ($R = 0.70$). One explanation is that the thermal decomposition of OA in CV could vary among different instruments, but the aging trends are similar between SV- and CV-AMS.

3.4 Coal combustion

Coal combustion emission is one of the most important primary sources of OA in winter in north China ~~(Sun et al., 2013)~~(Sun et al., 2013). Although CCOA was resolved and quantified by SV-AMS in several previous studies ~~(Sun et al., 2016a;Hu et al., 2013)~~(Sun et al., 2016a;Hu et al., 2013), it becomes more challenging to separate it from traffic-related HOA in megacities of China due to their relatively similar mass spectra and diurnal variations. By burning two different types of coals, i.e., brown and bituminous coals under flaming and smoldering conditions, we found that the differences in CCOA spectra of SV-AMS can be substantial under different burning conditions, while the spectra are relatively similar under smoldering conditions ($R^2 = 0.98$, Fig. ~~2~~5). Consistent with previously resolved CCOA in ambient aerosol, the CCOA source spectra are all characterized by prominent hydrocarbons ions (for example, m/z 41, m/z 43, m/z 55 and m/z 57), and PAHs-related fragments, e.g., m/z 152, m/z 165, m/z 178, m/z 189, m/z 202, m/z 215, etc. It is interesting to note that the CCOA spectrum in Beijing ~~(Sun et al., 2016a)~~(Sun et al., 2016a) resembles more that of flaming combustion of bituminous coal, while that observed at Changdao island in central eastern China ~~(Hu et al., 2013)~~(Hu et al., 2013) shows more similarity to that of smoldering combustion of bituminous coal. This is consistent with the fact that the bituminous coal accounted for ~78% of the total coal production according to the China Coal Industry Yearbook ~~(Zhou et al., 2016)~~(Zhou et al., 2016), yet the CCOA emissions can be different in different areas due to different combustion conditions. We also noticed that the signals of m/z's >150 contribute approximately ~40% of the total signal of CCOA measured by SV-AMS (Fig. S8), which is much higher than those in crop straw/wood burning and cooking emissions, suggesting that CCOA contains much higher fractions of high molecular weight

organic compounds, e.g., PAHs. Therefore, source apportionment studies in regions with large influences of coal combustion emissions needs to be cautious. For example, PMF analysis of high-resolution mass spectra of OA by limiting m/z to 150 could underestimate CCOA substantially. Considering that the contribution of CCOA to OA is ~20% during wintertime in Beijing (Sun et al., 2016a)(Sun et al., 2016a), the missed m/z's > 150 in PMF analysis could cause an underestimation of coal

5   combustion by ~8%.

Similar to COA and BBOA, the CCOA spectra of CV-ACSM resemble those of SV-AMS (Fig. S6), yet with much higher f_{44}. Although the thermal decomposition and the increased residence time in CV result in the larger molecular-weight fragments shifting towards smaller ions, the PAHs signals are well retained in the mass spectra of CV-ACSM (e.g., m/z 152, m/z 165, m/z 178, m/z 189, m/z 202, m/z 215) due to the stabilized chemical structures of PAHs that are very resistant to fragmentation after

10   ionization (McLafferty and Turecek, 1993)(McLafferty and Turecek, 1993)., consistent with the observations of PAHs from burning different types of coals (Zheng et al., 2020). These results indicate that PAHs can also be used as tracers to identify the coal combustion OA measured by CV-ACSM. We also observed the differences in f_{44} produced from flaming and smoldering combustion. While the flaming combustion of brown coal produced higher f_{44} than smoldering for both SV-AMS and CV-ACSM (5.7% vs. 2.9%, and 3.2% vs. 1.7%, respectively), it was reversed for bituminous coal burning. Previous studies

15   showed that the CCOA spectra evolved during the combustion process depending on the burning temperature and oxygen supplied (Wang et al., 2013)(Wang et al., 2013). In addition, f_{60} was only observed to be significant in smoldering combustion of bituminous coal (0.46%, Fig. S3), suggesting that coal combustion can be a potential source of levoglucosan. For instance, Yan et al. (2018)For instance, Yan et al. (2018) observed the emissions of levoglucosan from semi-anthracite burning while medium- and high-volatile bituminous coals appear to be negligible sources.

20   The O/C ratios of coal combustion OA are generally low ranging from 0.08 to 0.23, which are close to those (0.14 – 0.22) identified in ambient air in winter and spring (Xu et al., 2019;Sun et al., 2016a;Hu et al., 2013)(Xu et al., 2019;Sun et al., 2016a;Hu et al., 2013). The low O/C ratios suggest relatively low water solubility of CCOA. Indeed, the WSOC from the four different coal combustion on average accounted for 16 – 34% of the total OC with the flaming combustion generating more water-soluble organic compounds (24 – 34%). As a result, the O/C ratios of water-soluble CCOA are approximately twice that

25   of CCOA, and consistently, the contributions of oxygenated ions (36.9 – 49.7%) are much higher. As shown in Fig. S3, the mass spectra of water-soluble CCOA are quite different from the total CCOA, especially for flaming combustion of bituminous coal (R^2=0.24). Although the signals of high m/z's are largely decreased in the mass spectra of water-soluble CCOA, the spectral characteristics of PAHs (e.g., m/z 115, 128, 139, 152, 165, 181 etc.) are still observed (Fig. S9). Because of the reduced signals for large m/z's, the spectral correlations between water-soluble CCOA and other water-soluble primary OA are much

30   elevated (Fig. 25), increasing the difficulties for the identification of water-soluble CCOA. For example, the spectrum of water-soluble CCOA identified in winter in our previous study was much different from those measured in this study (Qiu et al.,

2019)(Qiu et al., 2019), and the O/C ratio (0.68) was also much higher. One reason is likely due to the aging of CCOA during the transport to Beijing because of the ban of coal burning in the city. The uncertainties in PMF analysis caused by the spectra could be another possibility.

4 Conclusion and Implications

5   Aerodyne AMS and ACSM have been widely used to measure OA worldwide, and the subsequent source apportionment of OA by PMF or ME-2 relies largely upon the mass spectral profiles of primary emissions. While the mass spectra of primary emissions, e.g., cooking, biomass burning, and traffic are relatively well characterized by SV-AMS, their behaviors in the newly developed CV-AMS/ACSM are poorly known. Considering the rapid increases in deployments of CV-ACSM and the studies in water-soluble OA worldwide, it is critical importance to further characterize the mass spectra of primary emissions

10   with CV-ACSM for a better source apportionment of OA in the future. In addition, the mass spectra of OA from coal combustion emissions, one of the most important primary sources in winter in China, are rarely characterized. By measuring 21 different primary emissions with SV-AMS and CV-ACSM, the similar spectral characteristics of primary OA between CV-ACSM and SV-AMS are demonstrated, yet the changes in specific marker m/z's (e.g., $f_{44}, f_{43}, f_{60}, f_{73}$, etc.) and m/z ratios (f_{55}/f_{57}, $f_{41}/f_{43}, f_{60}/f_{73}$, etc.) for source diagnostics are also observed due to additional thermal decomposition in CV. Among all primary

15   emissions, we found that the COA spectrum is the most robust for both SV-AMS and CV-ACSM, and has no clear dependence on oil gradients. However, the spectral differences between water-soluble OA and the total OA can be substantial for both SV-AMS and CV-ACSM depending on water solubility which is in the order of BBOA > WBOA > COA > CCOA. Noted that the mass loadings of primary emissions in this experiment are much higher than those in ambient air, which could cause some differences in water solubility and subsequent spectral differences in WSOA. In addition, we found that mass spectra of WSOA

20   from CV-ACSM are relatively well correlated among different primary emissions, highlighting the challenges in source apportionment of WSOA using CV-ACSM in the future.

We further demonstrate the importance of mass spectra of primary emissions for OA source apportionment in a field campaign that was conducted with a $PM_{2.5}$ CV-ACSM at a highly polluted rural site in North China Plain in winter.(Kuang et al., 2019) (Kuang et al., 2020). Positive matrix factorization of OA was able to identify four primary OA factors including traffic-related

25   HOA, COA, BBOA and CCOA, and one secondary OOA. We found that the average contributions of HOA and COA (19% and 16%, respectively) were much higher than expected because the rural site is far from urban areas (~15 km) and tends to have small influences from cooking and traffic emissions. Although the temporal variations appeared to be reasonable and were correlated with specific tracer species (e.g., BC and CO), the COA spectrum showed unrealistically higher m/z 27 and m/z 29, and BBOA and CCOA spectra showed much lower f_{44} than those observed in source profiles (Fig. 47). Therefore, we

30   reperformed the OA source apportionment with ME-2 by constraining four primary OA factors. Considering the chemical

environment of sampling site, we used the average mass spectra of COA from vegetable oil, flaming combustion of bituminous coal, crop straw burning of corn, and HOA resolved in Rizhao city by the same CV-ACSM as in this study in September ~~(Lei et al., 2019)~~(Lei et al., 2019) as constrains in ME-2 analysis with a-value ranging from 0 to 0.3. As shown in Fig. 4~~7~~, the ME-2 results showed much reduced HOA and COA contributions (8% and 5%, respectively) compared with those from PMF analysis. As a result, BBOA and CCOA became the two major primary sources at the rural site in North China Plain (32% and 21%, respectively), consistent with the fact that coal and crop straw are the major fuels for residential heating. Also, the unrealistically high morning COA peak in PMF analysis was disappeared in the ME-2 analysis further supporting the rationale of ME-2 results (Fig. 4~~7~~). Although the average contributions of POA and SOA are very close with and without constraining POA spectral profiles, the apportionment of POA factors can be improved substantially. The accurate source apportionment results have significant implications for future air pollution mitigating strategies, for instance, our new results highlight that reducing coal combustion and biomass burning emissions would be the most effective measure to improve the winter air quality in rural areas in North China Plain.

Data availability. The data in this study are available from the authors upon request (sunyele@mail.iap.ac.cn).

Author contributions. YS, QW and YH designed the research. QW, YH, YQ, CC, LL, and ZL conducted the experiments. LL, QW, YH and YQ analyzed the data. YJ, PF, ZW and DW reviewed and commented on the paper. QW, YH, and YS wrote the paper.

Competing interests. The authors declare that they have no conflict of interest.

References

Alfarra, M. R., Prevot, A. S. H., Szidat, S., Sandradewi, J., Weimer, S., Lanz, V. A., Schreiber, D., Mohr, M., and Baltensperger, U.: Identification of the mass spectral signature of organic aerosols from wood burning emissions, Environ. Sci. Technol., 41, 5770-5777, 2007.

Allan, J. D., Williams, P. I., Morgan, W. T., Martin, C. L., Flynn, M. J., Lee, J., Nemitz, E., Phillips, G. J., Gallagher, M. W., and Coe, H.: Contributions from transport, solid fuel burning and cooking to primary organic aerosols in two UK cities, Atmos. Chem. Phys., 10, 647-668, 2010.

Bahreini, R., Ervens, B., Middlebrook, A. M., Warneke, C., de Gouw, J. A., DeCarlo, P. F., Jimenez, J. L., Brock, C. A., Neuman,

J. A., Ryerson, T. B., Stark, H., Atlas, E., Brioude, J., Fried, A., Holloway, J. S., Peischl, J., Richter, D., Walega, J., Weibring, P., Wollny, A. G., and Fehsenfeld, F. C.: Organic aerosol formation in urban and industrial plumes near Houston and Dallas, Texas, J. Geophys. Res.-Atmos., 114, 10.1029/2008jd011493, 2009.

Bottenus, C. L. H., Massoli, P., Sueper, D., Canagaratna, M. R., VanderSchelden, G., Jobson, B. T., and VanReken, T. M.: Identification of amines in wintertime ambient particulate material using high resolution aerosol mass spectrometry, Atmos. Environ., 180, 173-183, 10.1016/j.atmosenv.2018.01.044, 2018.

Bozzetti, C., El Haddad, I., Salameh, D., Daellenbach, K. R., Fermo, P., Gonzalez, R., Cruz Minguillon, M., Iinuma, Y., Poulain, L., Elser, M., Mueller, E., Slowik, J. G., Jaffrezo, J.-L., Baltensperger, U., Marchand, N., and Prevot, A. S. H.: Organic aerosol source apportionment by offline-AMS over a full year in Marseille, Atmos. Chem. Phys., 17, 8247-8268, 10.5194/acp-17-8247-2017, 2017.

Canagaratna, M., Jayne, J., Jimenez, J. L., Allan, J. A., Alfarra, R., Zhang, Q., Onasch, T., Drewnick, F., Coe, H., Middlebrook, A., Delia, A., Williams, L., Trimborn, A., Northway, M., Kolb, C., Davidovits, P., and Worsnop, D.: Chemical and microphysical characterization of aerosols via Aerosol Mass Spectrometry, Mass Spectrom. Rev., 26, 185-222, 2007.

Canagaratna, M. R., Jayne, J. T., Ghertner, D. A., Herndon, S., Shi, Q., Jimenez, J. L., Silva, P. J., Williams, P., Lanni, T., Drewnick, F., Demerjian, K. L., Kolb, C. E., and Worsnop, D. R.: Chase studies of particulate emissions from in-use New York City vehicles, Aerosol Sci. Tech., 38, 555-573, 2004.

Canagaratna, M. R., Jimenez, J. L., Kroll, J. H., Chen, Q., Kessler, S. H., Massoli, P., Hildebrandt Ruiz, L., Fortner, E., Williams, L. R., Wilson, K. R., Surratt, J. D., Donahue, N. M., Jayne, J. T., and Worsnop, D. R.: Elemental ratio measurements of organic compounds using aerosol mass spectrometry: characterization, improved calibration, and implications, Atmos. Chem. Phys., 15, 253-272, 10.5194/acp-15-253-2015, 2015.

Chen, J., Li, C., Ristovski, Z., Milic, A., Gu, Y., Islam, M. S., Wang, S., Hao, J., Zhang, H., and He, C.: A review of biomass burning: Emissions and impacts on air quality, health and climate in China, Sci. Total Environ., 579, 1000-1034, 2017.

Collier, S., Zhou, S., Kuwayama, T., Forestieri, S., Brady, J., Zhang, M., Kleeman, M., Cappa, C., Bertram, T., and Zhang, Q.: Organic PM Emissions from Vehicles: Composition, O/C Ratio, and Dependence on PM Concentration, Aerosol Sci. Tech., 49, 86-97, 10.1080/02786826.2014.1003364, 2015.

Collier, S., Zhou, S., Onasch, T. B., Jaffe, D. A., Kleinman, L., Sedlacek, A. J., Briggs, N. L., Hee, J., Fortner, E., Shilling, J. E., Worsnop, D., Yokelson, R. J., Parworth, C., Ge, X., Xu, J., Butterfield, Z., Chand, D., Dubey, M. K., Pekour, M. S., Springston, S., and Zhang, Q.: Regional Influence of Aerosol Emissions from Wildfires Driven by Combustion Efficiency: Insights from the BBOP Campaign, Environ. Sci. Technol., 50, 8613-8622, 10.1021/acs.est.6b01617, 2016.

Cubison, M. J., Ortega, A. M., Hayes, P. L., Farmer, D. K., Day, D., Lechner, M. J., Brune, W. H., Apel, E., Diskin, G. S., Fisher, J. A., Fuelberg, H. E., Hecobian, A., Knapp, D. J., Mikoviny, T., Riemer, D., Sachse, G. W., Sessions, W., Weber, R. J., Weinheimer, A. J., Wisthaler, A., and Jimenez, J. L.: Effects of aging on organic aerosol from open biomass burning smoke in aircraft and laboratory studies, Atmos. Chem. Phys., 11, 12049-12064, 10.5194/acp-11-12049-2011, 2011.

Daellenbach, K. R., Bozzetti, C., Krepelova, A. K., Canonaco, F., Wolf, R., Zotter, P., Fermo, P., Crippa, M., Slowik, J. G., Sosedova, Y., Zhang, Y., Huang, R. J., Poulain, L., Szidat, S., Baltensperger, U., El Haddad, I., and Prevot, A. S. H.:

Characterization and source apportionment of organic aerosol using offline aerosol mass spectrometry, Atmospheric Measurement Techniques, 9, 23-39, 10.5194/amt-9-23-2016, 2016.

Desyaterik, Y., Sun, Y., Shen, X., Lee, T., Wang, X., Wang, T., and Collett Jr., J. L.: Speciation of "brown" carbon in cloud water impacted by agricultural biomass burning in eastern China, Journal of Geophysical Research: Atmospheres, 118, 7389-7399, 10.1002/jgrd.50561, 2013.

Donahue, N. M., Robinson, A. L., Stanier, C. O., and Pandis, S. N.: Coupled partitioning, dilution, and chemical aging of semivolatile organics, Environ. Sci. Technol., 40, 2635-2643, 2006.

Faber, P., Drewnick, F., Veres, P. R., Williams, J., and Borrmann, S.: Anthropogenic sources of aerosol particles in a football stadium: Real-time characterization of emissions from cigarette smoking, cooking, hand flares, and color smoke bombs by high-resolution aerosol mass spectrometry, Atmos. Environ., 77, 1043-1051, 10.1016/j.atmosenv.2013.05.072, 2013.

Fang, Z., Deng, W., Zhang, Y. L., Ding, X., Tang, M. J., Liu, T. Y., Hu, Q. H., Zhu, M., Wang, Z. Y., Yang, W. Q., Huang, Z. H., Song, W., Bi, X. H., Chen, J. M., Sun, Y. L., George, C., and Wang, X. M.: Open burning of rice, corn and wheat straws: primary emissions, photochemical aging, and secondary organic aerosol formation, Atmos. Chem. Phys., 17, 14821-14839, 10.5194/acp-17-14821-2017, 2017.

Gilardoni, S., Massoli, P., Paglione, M., Giulianelli, L., Carbone, C., Rinaldi, M., Decesari, S., Sandrini, S., Costabile, F., Gobbi, G. P., Pietrogrande, M. C., Visentin, M., Scotto, F., Fuzzi, S., and Facchini, M. C.: Direct observation of aqueous secondary organic aerosol from biomass-burning emissions, Proc. Natl. Acad. Sci. U. S. A., 113, 10013-10018, 10.1073/pnas.1602212113, 2016.

He, L. Y., Lin, Y., Huang, X. F., Guo, S., Xue, L., Su, Q., Hu, M., Luan, S. J., and Zhang, Y. H.: Characterization of high-resolution aerosol mass spectra of primary organic aerosol emissions from Chinese cooking and biomass burning, Atmos. Chem. Phys., 10, 11535-11543, 10.5194/acp-10-11535-2010, 2010.

He, Y., Sun, Y., Kuang, Y., Wang, Q., Zhao, P., Cheng, Y., Zhao, G., Tao, J., Ma, N., Su, H., and Zhang, Y.: Fine particle characterization in North China Plain (NCP), in preparation, in preparation.

Hennigan, C. J., Sullivan, A. P., Collett, J. L., and Robinson, A. L.: Levoglucosan stability in biomass burning particles exposed to hydroxyl radicals, Geophys. Res. Lett., 37, L09806, doi:10.1029/2010GL043088, 2010.

Hennigan, C. J., Miracolo, M. A., Engelhart, G. J., May, A. A., Presto, A. A., Lee, T., Sullivan, A. P., McMeeking, G. R., Coe, H., Wold, C. E., Hao, W. M., Gilman, J. B., Kuster, W. C., de Gouw, J., Schichtel, B. A., J. L. Collett, J., Kreidenweis, S. M., and Robinson, A. L.: Chemical and physical transformations of organic aerosol from the photo-oxidation of open biomass burning emissions in an environmental chamber, Atmos. Chem. Phys., 11, 7669-7686, 10.5194/acp-11-7669-2011, 2011.

Hu, W., Campuzano-Jost, P., Day, D. A., Croteau, P., Canagaratna, M. R., Jayne, J. T., Worsnop, D. R., and Jimenez, J. L.: Evaluation of the new capture vaporizer for aerosol mass spectrometers (AMS) through field studies of inorganic species, Aerosol Sci. Tech., 51, 735–754, 10.1080/02786826.2017.1296104, 2017.
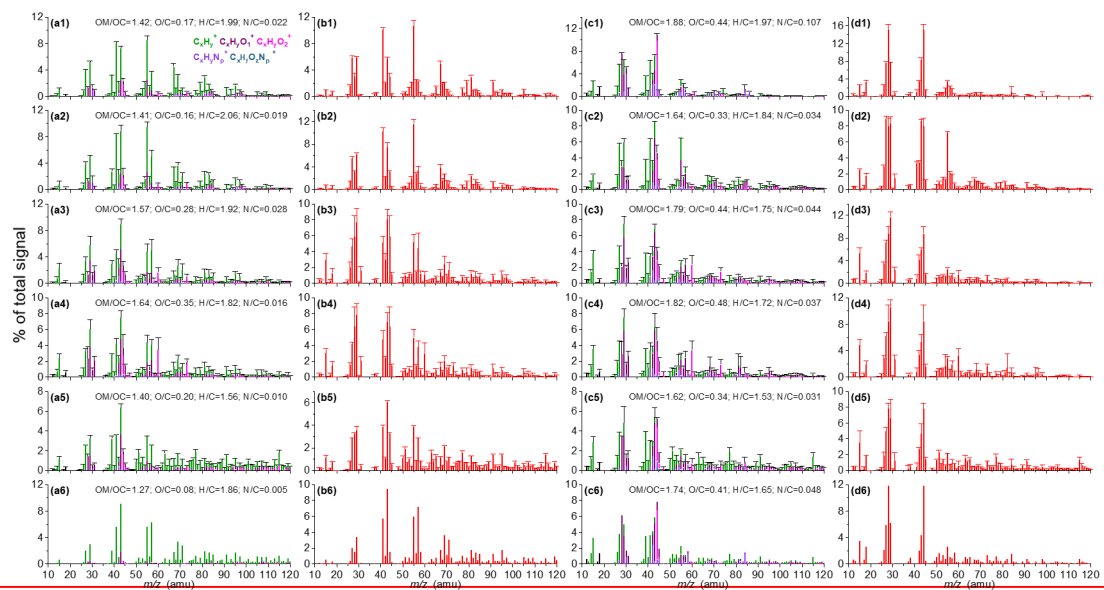
Hu, W., Day, D. A., Campuzano-Jost, P., Nault, B. A., Park, T., Lee, T., Croteau, P., Canagaratna, M. R., Jayne, J. T., Worsnop, D. R., and Jimenez, J. L.: Evaluation of the new capture vaporizer for aerosol mass spectrometers: Characterization of organic aerosol mass spectra, Aerosol Sci. Tech., 52, 725-739, 10.1080/02786826.2018.1454584, 2018a.

Hu, W., Day, D. A., Campuzano-Jost, P., Nault, B. A., Park, T., Lee, T., Croteau, P., Canagaratna, M. R., Jayne, J. T., Worsnop, D. R., and Jimenez, J. L.: Evaluation of the New Capture Vaporizer for Aerosol Mass Spectrometers (AMS): Elemental Composition and Source Apportionment of Organic Aerosols (OA), ACS Earth and Space Chemistry, 2, 410-421, 10.1021/acsearthspacechem.8b00002, 2018b.

Hu, W. W., Hu, M., Yuan, B., Jimenez, J. L., Tang, Q., Peng, J. F., Hu, W., Shao, M., Wang, M., Zeng, L. M., Wu, Y. S., Gong, Z. H., Huang, X. F., and He, L. Y.: Insights on organic aerosol aging and the influence of coal combustion at a regional receptor site of central eastern China, Atmos. Chem. Phys., 13, 10095-10112, 10.5194/acp-13-10095-2013, 2013.

Huffman, J. A., Jayne, J. T., Drewnick, F., Aiken, A. C., Onasch, T., Worsnop, D. R., and Jimenez, J. L.: Design, modeling, optimization, and experimental tests of a particle beam width probe for the Aerodyne Aerosol Mass Spectrometer, Aerosol Sci. Tech., 39, 1143-1163, 2005.

Kaltsonoudis, C., Kostenidou, E., Louvaris, E., Psichoudaki, M., Tsiligiannis, E., Florou, K., Liangou, A., and Pandis, S. N.: Characterization of fresh and aged organic aerosol emissions from meat charbroiling, Atmos. Chem. Phys., 17, 7143-7155, 10.5194/acp-17-7143-2017, 2017.

Kuang, Y., He, Y., Xu, W., ~~Sun, Y.,~~ Zhao, P., Cheng, Y., Zhao, G., Tao, J., Ma, N., Su, H., and Zhang, Y~~., Sun, J., Cheng, P., Yang, W., Zhang, S., Wu, C., and Zhao, C~~.: Distinct diurnal variation ~~of~~in organic aerosol hygroscopicity and its relationship with oxygenated organic aerosol, Atmos. Chem. Phys~~. Discuss., 2019, 1-33, 10.5194/acp-2019-633, 2019~~., 20, 865-880, 2020.

Laskin, A., Smith, J. S., and Laskin, J.: Molecular characterization of nitrogen-containing organic compounds in biomass burning aerosols using high-resolution mass spectrometry, Environ. Sci. Technol., 43, 3764-3771, doi:10.1021/es803456n, 2009.

Lee, T., Sullivan, A. P., Mack, L., Jimenez, J. L., Kreidenweis, S. M., Onasch, T. B., Worsnop, D. R., Malm, W., Wold, C. E., Hao, W. M., and Collett, J. L.: Chemical Smoke Marker Emissions During Flaming and Smoldering Phases of Laboratory Open Burning of Wildland Fuels, Aerosol Sci. Tech., 44, 1-5, 2010.

Lei, L., Xie, C., Wang, D., He, Y., Wang, Q., Zhou, W., Hu, W., Fu, P., Chen, Y., Pan, X., Wang, Z., Worsnop, D. R., and Sun, Y.: Fine particle characterization in a coastal city in China: composition, sources, and impacts of industrial emissions, Atmos. Chem. Phys. Discuss., 2019, 1-24, 10.5194/acp-2019-854, 2019.

Li, L. J., Ren, L. J., Ren, H., Yue, S. Y., Xie, Q. R., Zhao, W. Y., Kang, M. J., Li, J., Wang, Z. F., Sun, Y. L., and Fu, P. Q.: Molecular Characterization and Seasonal Variation in Primary and Secondary Organic Aerosols in Beijing, China, J. Geophys. Res.-Atmos., 123, 12394-12412, 10.1029/2018jd028527, 2018.

Li, Y. J., Sun, Y., Zhang, Q., Li, X., Li, M., Zhou, Z., and Chan, C. K.: Real-time chemical characterization of atmospheric particulate matter in China: A review, Atmos. Environ., 158, 270-304, 10.1016/j.atmosenv.2017.02.027, 2017.

Lin, C., Ceburnis, D., Hellebust, S., Buckley, P., Wenger, J., Canonaco, F., Prévôt, A. S. H., Huang, R.-J., O'Dowd, C., and Ovadnevaite, J.: Characterization of Primary Organic Aerosol from Domestic Wood, Peat, and Coal Burning in Ireland, Environ. Sci. Technol., 51, 10624-10632, 10.1021/acs.est.7b01926, 2017.

Liu, T., Wang, Z., Wang, X., and Chan, C. K.: Primary and secondary organic aerosol from heated cooking oil emissions,

Atmos. Chem. Phys., 18, 11363-11374, 10.5194/acp-18-11363-2018, 2018.

Liu, T. Y., Li, Z. J., Chan, M. N., and Chan, C. K.: Formation of secondary organic aerosols from gas-phase emissions of heated cooking oils, Atmos. Chem. Phys., 17, 7333-7344, 10.5194/acp-17-7333-2017, 2017.

Matthew, B. M., Middlebrook, A. M., and Onasch, T. B.: Collection Efficiencies in an Aerodyne Aerosol Mass Spectrometer as a Function of Particle Phase for Laboratory Generated Aerosols, Aerosol Sci. Tech., 42, 884 - 898, 2008.

Mayol-Bracero, O. L., Guyon, P., Graham, B., Roberts, G., Andreae, M. O., Decesari, S., Facchini, M. C., Fuzzi, S., and Artaxo, P.: Water-soluble organic compounds in biomass burning aerosols over Amazonia - 2. Apportionment of the chemical composition and importance of the polyacidic fraction, J. Geophys. Res.-Atmos., 107, 8091, 2002.

McLafferty, F. W., and Turecek, F.: Interpretation of Mass Spectra, University Science Books, Mill Valley, California, 1993.

Middlebrook, A. M., Bahreini, R., Jimenez, J. L., and Canagaratna, M. R.: Evaluation of Composition-Dependent Collection Efficiencies for the Aerodyne Aerosol Mass Spectrometer using Field Data, Aerosol Sci. Tech., 46, 258-271, 10.1080/02786826.2011.620041, 2012.

Mohr, C., Huffman, J. A., Cubison, M. J., Aiken, A. C., Docherty, K. S., Kimmel, J. R., Ulbrich, I. M., Hannigan, M., and Jimenez, J. L.: Characterization of primary organic aerosol emissions from meat cooking, trash burning, and motor vehicles with High-Resolution Aerosol Mass Spectrometry and comparison with ambient and chamber observations, Environ. Sci. Technol., 43, 2443-2449, doi:10.1021/es8011518, 2009.

Mohr, C., Richter, R., DeCarlo, P. F., Prévôt, A. S. H., and Baltensperger, U.: Spatial variation of chemical composition and sources of submicron aerosol in Zurich during wintertime using mobile aerosol mass spectrometer data, Atmos. Chem. Phys., 11, 7465-7482, 10.5194/acp-11-7465-2011, 2011.

Mohr, C., DeCarlo, P. F., Heringa, M. F., Chirico, R., Slowik, J. G., Richter, R., Reche, C., Alastuey, A., Querol, X., Seco, R., Peñuelas, J., Jiménez, J. L., Crippa, M., Zimmermann, R., Baltensperger, U., and Prévôt, A. S. H.: Identification and quantification of organic aerosol from cooking and other sources in Barcelona using aerosol mass spectrometer data, Atmos. Chem. Phys., 12, 1649-1665, 10.5194/acp-12-1649-2012, 2012.

Morgan, W. T., Allan, J. D., Bauguitte, S., Darbyshire, E., Flynn, M. J., Lee, J., Liu, D., Johnson, B., Haywood, J., and Longo, K. M.: Transformation and ageing of biomass burning carbonaceous aerosol over tropical South America from aircraft in situ measurements during SAMBBA, 2020.

Paatero, P., and Tapper, U.: Positive matrix factorization: A non-negative factor model with optimal utilization of error estimates of data values, Environmetrics, 5, 111-126, 1994.

Paatero, P.: The multilinear engine - A table-driven, least squares program for solving multilinear problems, including the n-way parallel factor analysis model, Journal of Computational and Graphical Statistics, 8, 854-888, 1999.

Qiu, Y., Xie, Q., Wang, J., Xu, W., Li, L., Wang, Q., Zhao, J., Chen, Y., Chen, Y., Wu, Y., Du, W., Zhou, W., Lee, J., Zhao, C., Ge, X., Fu, P., Wang, Z., Worsnop, D. R., and Sun, Y.: Vertical Characterization and Source Apportionment of Water-Soluble Organic Aerosol with High-resolution Aerosol Mass Spectrometry in Beijing, China, ACS Earth and Space Chemistry, 10.1021/acsearthspacechem.8b00155, 2019.

Reyes-Villegas, E., Bannan, T., Le Breton, M., Mehra, A., Priestley, M., Percival, C., Coe, H., and Allan, J. D.: Online Chemical

Characterization of Food-Cooking Organic Aerosols: Implications for Source Apportionment, Environ. Sci. Technol., 52, 5308-5318, 10.1021/acs.est.7b06278, 2018a.

Reyes-Villegas, E., Priestley, M., Ting, Y. C., Haslett, S., Bannan, T., Le Breton, M., Williams, P. I., Bacak, A., Flynn, M. J., Coe, H., Percival, C., and Allan, J. D.: Simultaneous aerosol mass spectrometry and chemical ionisation mass spectrometry measurements during a biomass burning event in the UK: insights into nitrate chemistry, Atmos. Chem. Phys., 18, 4093-4111, 10.5194/acp-18-4093-2018, 2018b.

Robinson, E. S., Gu, P. S., Ye, Q., Li, H. Z., Shah, R. U., Apte, J. S., Robinson, A. L., and Presto, A. A.: Restaurant Impacts on Outdoor Air Quality: Elevated Organic Aerosol Mass from Restaurant Cooking with Neighborhood-Scale Plume Extents, Environ. Sci. Technol., 52, 9285-9294, 10.1021/acs.est.8b02654, 2018.

Schauer, J. J., Kleeman, M. J., Cass, G. R., and Simoneit, B. R. T.: Measurement of emissions from air pollution sources. 4. C-1-C-27 organic compounds from cooking with seed oils, Environ. Sci. Technol., 36, 567-575, 2002.

Schneider, J., Weimer, S., Drewnick, F., Borrmann, S., Helas, G., Gwaze, P., Schmid, O., Andreae, M. O., and Kirchner, U.: Mass spectrometric analysis and aerodynamic properties of various types of combustion-related aerosol particles, Int. J. Mass Spectrom., 258, 37-49, 2006.

Shilling, J. E., Chen, Q., King, S. M., Rosenoern, T., Kroll, J. H., Worsnop, D. R., DeCarlo, P. F., Aiken, A. C., Sueper, D., Jimenez, J. L., and Martin, S. T.: Loading-dependent elemental composition of a-pinene SOA particles, Atmos. Chem. Phys., 9, 771-782, 2009.

Sun, Y., Du, W., Fu, P., Wang, Q., Li, J., Ge, X., Zhang, Q., Zhu, C., Ren, L., Xu, W., Zhao, J., Han, T., Worsnop, D. R., and Wang, Z.: Primary and secondary aerosols in Beijing in winter: sources, variations and processes, Atmos. Chem. Phys., 16, 8309-8329, 10.5194/acp-16-8309-2016, 2016a.

Sun, Y., Jiang, Q., Xu, Y., Ma, Y., Zhang, Y., Liu, X., Li, W., Wang, F., Li, J., Wang, P., and Li, Z.: Aerosol characterization over the North China Plain: Haze life cycle and biomass burning impacts in summer, Journal of Geophysical Research: Atmospheres, 121, 2508-2521, 10.1002/2015jd024261, 2016b.

Sun, Y. L., Zhang, Q., Schwab, J. J., Demerjian, K. L., Chen, W. N., Bae, M. S., Hung, H. M., Hogrefe, O., Frank, B., Rattigan, O. V., and Lin, Y. C.: Characterization of the sources and processes of organic and inorganic aerosols in New York City with a high-resolution time-of-flight aerosol mass spectrometer, Atmos. Chem. Phys., 11, 1581-1602, 10.5194/acp-11-1581-2011, 2011.

Sun, Y. L., Wang, Z. F., Fu, P. Q., Yang, T., Jiang, Q., Dong, H. B., Li, J., and Jia, J. J.: Aerosol composition, sources and processes during wintertime in Beijing, China, Atmos. Chem. Phys., 13, 4577-4592, 10.5194/acp-13-4577-2013, 2013.

Wang, X., Williams, B., Wang, X., Tang, Y., Huang, Y., Kong, L., Yang, X., and Biswas, P.: Characterization of organic aerosol produced during pulverized coal combustion in a drop tube furnace, Atmos. Chem. Phys, 13, 10919-10932, 2013.

Wang, X. F., Gu, R. R., Wang, L. W., Xu, W. X., Zhang, Y. T., Chen, B., Li, W. J., Xue, L. K., Chen, J. M., and Wang, W. X.: Emissions of fine particulate nitrated phenols from the burning of five common types of biomass, Environ. Pollut., 230, 405-412, 10.1016/j.envpol.2017.06.072, 2017.

Weimer, S., Alfarra, M. R., Schreiber, D., Mohr, M., Prévôt, A. S. H., and Baltensperger, U.: Organic aerosol mass spectral

signatures from wood-burning emissions: Influence of burning conditions and wood type, J. Geophys. Res, 113, 2008.

Xu, L., Guo, H., Weber, R. J., and Ng, N. L.: Chemical Characterization of Water-Soluble Organic Aerosol in Contrasting Rural and Urban Environments in the Southeastern United States, Environ. Sci. Technol., 51, 78-88, 10.1021/acs.est.6b05002, 2017a.

Xu, W., Croteau, P., Williams, L., Canagaratna, M., Onasch, T., Cross, E., Zhang, X., Robinson, W., Worsnop, D., and Jayne, J.: Laboratory characterization of an aerosol chemical speciation monitor with PM2.5 measurement capability, Aerosol Sci. Tech., 51, 69-83, 10.1080/02786826.2016.1241859, 2017b.

Xu, W., Han, T., Du, W., Wang, Q., Chen, C., Zhao, J., Zhang, Y., Li, J., Fu, P., Wang, Z., Worsnop, D. R., and Sun, Y.: Effects of Aqueous-Phase and Photochemical Processing on Secondary Organic Aerosol Formation and Evolution in Beijing, China, Environ. Sci. Technol., 51, 762-770, 10.1021/acs.est.6b04498, 2017c.

Xu, W., Sun, Y., Wang, Q., Du, W., Zhao, J., Ge, X., Han, T., Zhang, Y., Zhou, W., Li, J., Fu, P., Wang, Z., and Worsnop, D. R.: Seasonal Characterization of Organic Nitrogen in Atmospheric Aerosols Using High Resolution Aerosol Mass Spectrometry in Beijing, China, ACS Earth and Space Chemistry, 10.1021/acsearthspacechem.7b00106, 2017d.

Xu, W., Sun, Y., Wang, Q., Zhao, J., Wang, J., Ge, X., Xie, C., Zhou, W., Du, W., Li, J., Fu, P., Wang, Z., Worsnop, D. R., and Coe, H.: Changes in Aerosol Chemistry From 2014 to 2016 in Winter in Beijing: Insights From High-Resolution Aerosol Mass Spectrometry, Journal of Geophysical Research: Atmospheres, 124, 1132-1147, doi:10.1029/2018JD029245, 2019.

Yan, C., Zheng, M., Sullivan, A. P., Shen, G., Chen, Y., Wang, S., Zhao, B., Cai, S., Desyaterik, Y., Li, X., Zhou, T., Gustafsson, Ö., and Collett, J. L.: Residential Coal Combustion as a Source of Levoglucosan in China, Environ. Sci. Technol., 52, 1665-1674, 10.1021/acs.est.7b05858, 2018.

Ye, Z., Liu, J., Gu, A., Feng, F., Liu, Y., Bi, C., Xu, J., Li, L., Chen, H., Chen, Y., Dai, L., Zhou, Q., and Ge, X.: Chemical characterization of fine particulate matter in Changzhou, China, and source apportionment with offline aerosol mass spectrometry, Atmos. Chem. Phys., 17, 2573-2592, 10.5194/acp-17-2573-2017, 2017.

Zhang, Q., Jimenez, J. L., Canagaratna, M. R., Allan, J. D., Coe, H., Ulbrich, I., Alfarra, M. R., Takami, A., Middlebrook, A. M., Sun, Y. L., Dzepina, K., Dunlea, E., Docherty, K., DeCarlo, P. F., Salcedo, D., Onasch, T., Jayne, J. T., Miyoshi, T., Shimono, A., Hatakeyama, S., Takegawa, N., Kondo, Y., Schneider, J., Drewnick, F., Weimer, S., Demerjian, K., Williams, P., Bower, K., Bahreini, R., Cottrell, L., R.J.Griffin, Rautiainen, J., Sun, J. Y., Zhang, Y. M., and Worsnop, D. R.: Ubiquity and dominance of oxygenated species in organic aerosols in anthropogenically-influenced northern hemisphere mid-latitudes, Geophys. Res. Lett., 34, L13801, doi:10.1029/2007GL029979, 2007.

Zheng, Y., Cheng, X., Liao, K., Li, Y., Li, Y., Huang, R. J., Hu, W., Liu, Y., Zhu, T., Chen, S., Zeng, L., Worsnop, D. R., and Chen, Q.: Characterization of Anthropogenic Organic Aerosols by TOF-ACSM with the New Capture Vaporizer, Atmos. Meas. Tech. Discuss., 2020, 1-24, 10.5194/amt-2019-449, 2020.

Zhou, W., Jiang, J. K., Duan, L., and Hao, J. M.: Evolution of Submicrometer Organic Aerosols during a Complete Residential Coal Combustion Process, Environ. Sci. Technol., 50, 7861-7869, 10.1021/acs.est.6b00075, 2016.
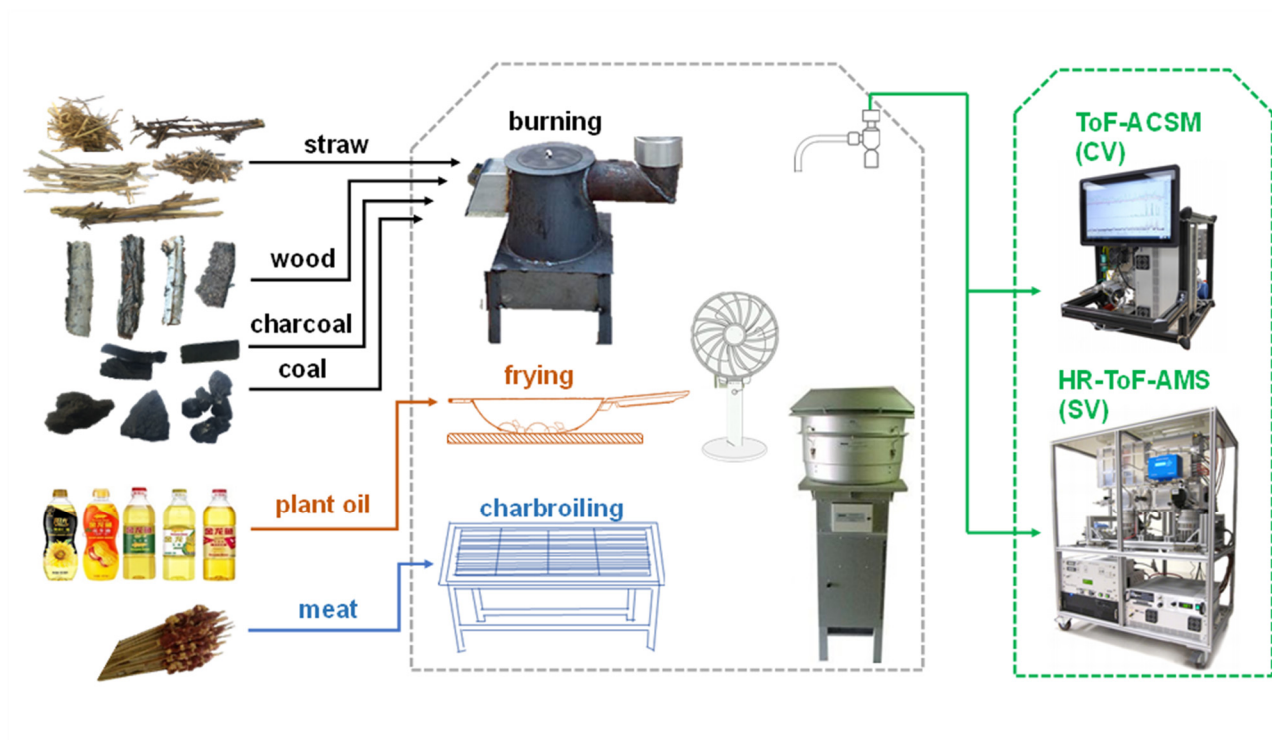
OM/OC=1.42; O/C=0.17; H/C=1.99; N/C=0.022
OM/OC=1.41; O/C=0.16; H/C=2.06; N/C=0.019
OM/OC=1.57; O/C=0.28; H/C=1.92; N/C=0.028
OM/OC=1.64; O/C=0.35; H/C=1.82; N/C=0.016
OM/OC=1.40; O/C=0.20; H/C=1.56; N/C=0.010
OM/OC=1.27; O/C=0.08; H/C=1.86; N/C=0.005
OM/OC=1.88; O/C=0.44; H/C=1.97; N/C=0.107
OM/OC=1.64; O/C=0.33; H/C=1.84; N/C=0.034
OM/OC=1.79; O/C=0.44; H/C=1.75; N/C=0.044
OM/OC=1.82; O/C=0.48; H/C=1.72; N/C=0.037
OM/OC=1.62; O/C=0.34; H/C=1.53; N/C=0.031
OM/OC=1.74; O/C=0.41; H/C=1.65; N/C=0.048

Figure 1. Schematic of cooking and burning experiments.

5
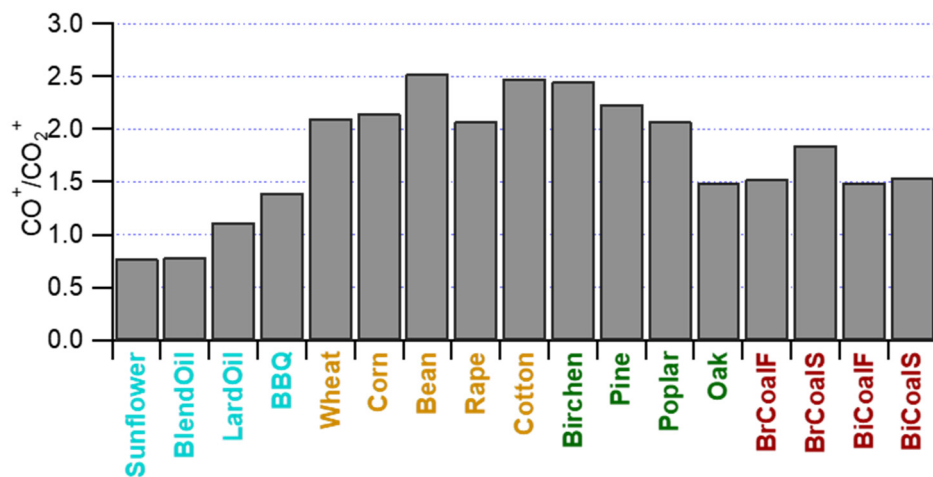
Figure 2. The ratio of measured CO^+/CO_2^+ for WSOA from 17 cooking and burning experiments.
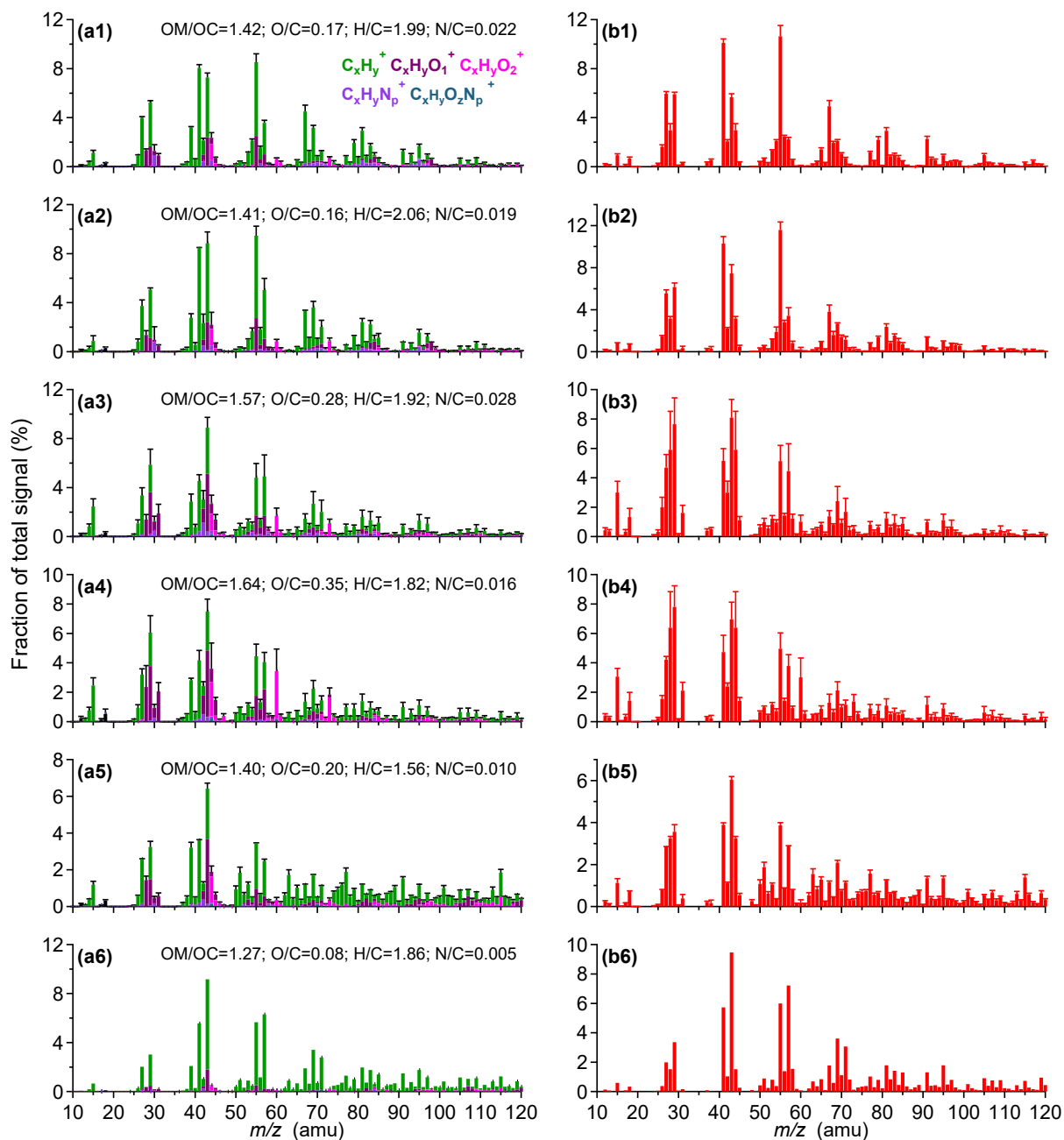
Figure 3. Average mass spectral profiles of OA measured by (a) SV-AMS, and (b) ~~CV-ACSM, and WSOA measured by (c) SV-AMS and (d)~~ CV-ACSM including (a1-d1) cooking emissions from vegetable oil, (a2-d2) from animal oil, (a3-d3) from crop straw burning, (a4-d4) from wood burning, and (a5-d5) and (a6-d6) from smoldering and flaming combustion of bituminous coal, respectively. The error bars represent one standard deviations. The elemental composition of OA and WSOA from SV-AMS are also shown. The detailed mass spectra for each cooking and burning are presented in Fig. S3.

21
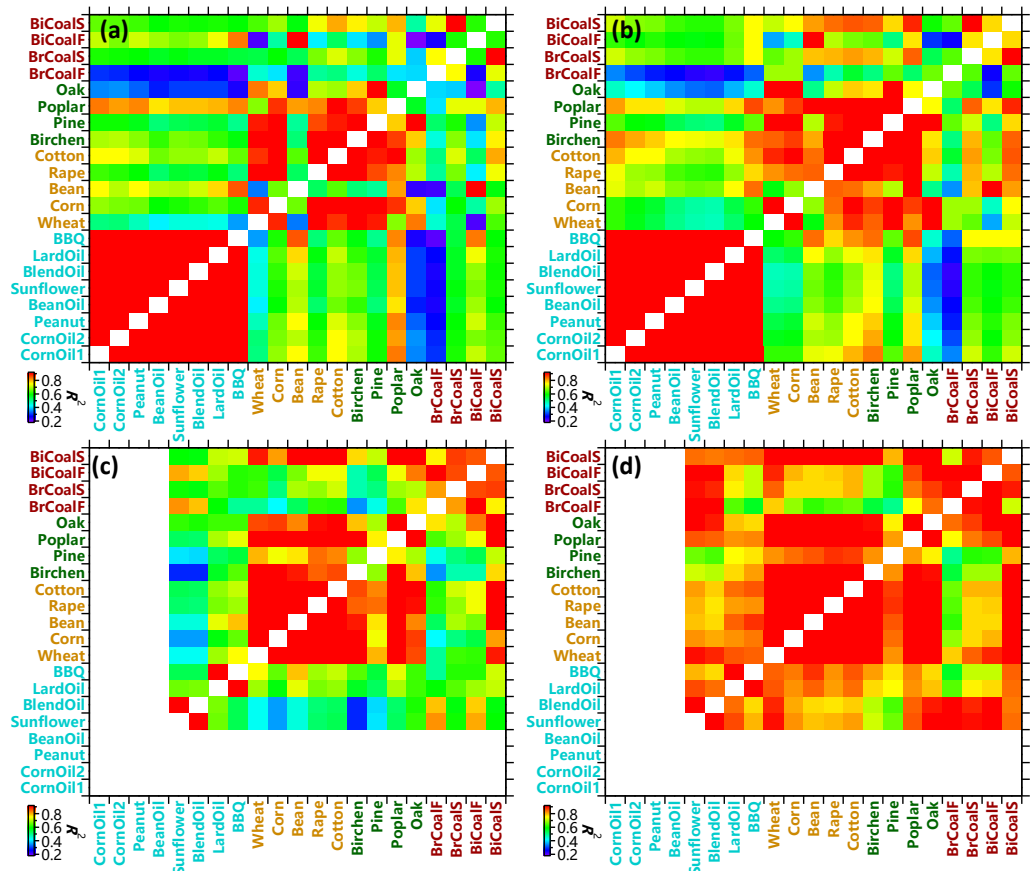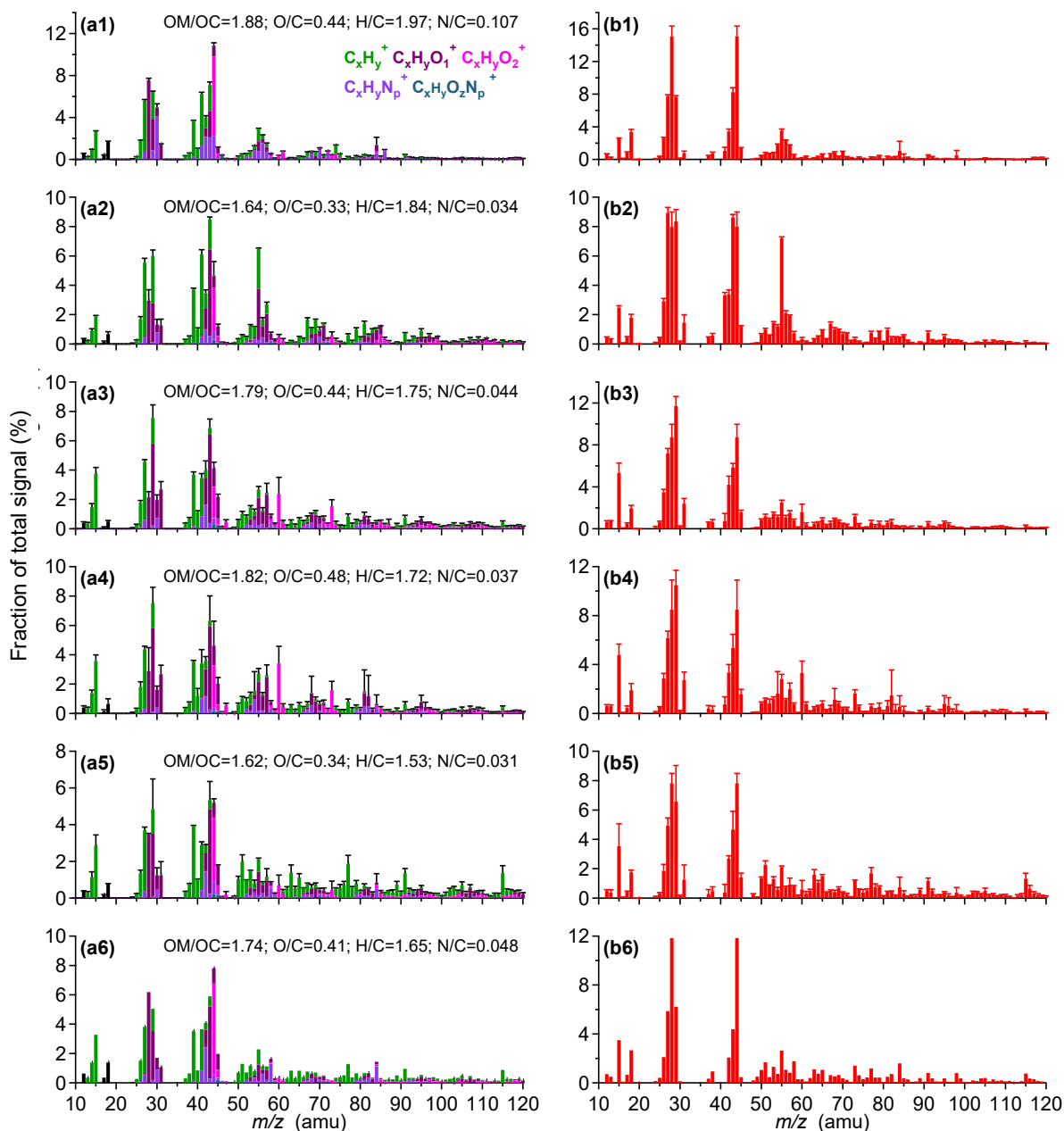
Figure 4. Average mass spectral profiles of WSOA measured by (a) SV-AMS and (b) CV-ACSM including (a1-d1) cooking emissions from vegetable oil, (a2-d2) from animal oil, (a3-d3) from crop straw burning, (a4-d4) from wood burning, and (a5-d5) and (a6-d6) from smoldering and flaming combustion of bituminous coal, respectively. The error bars represent one standard deviations. The elemental composition of OA and WSOA from SV-AMS are also shown. The detailed mass spectra for each cooking and burning are presented in Fig. S3.

23
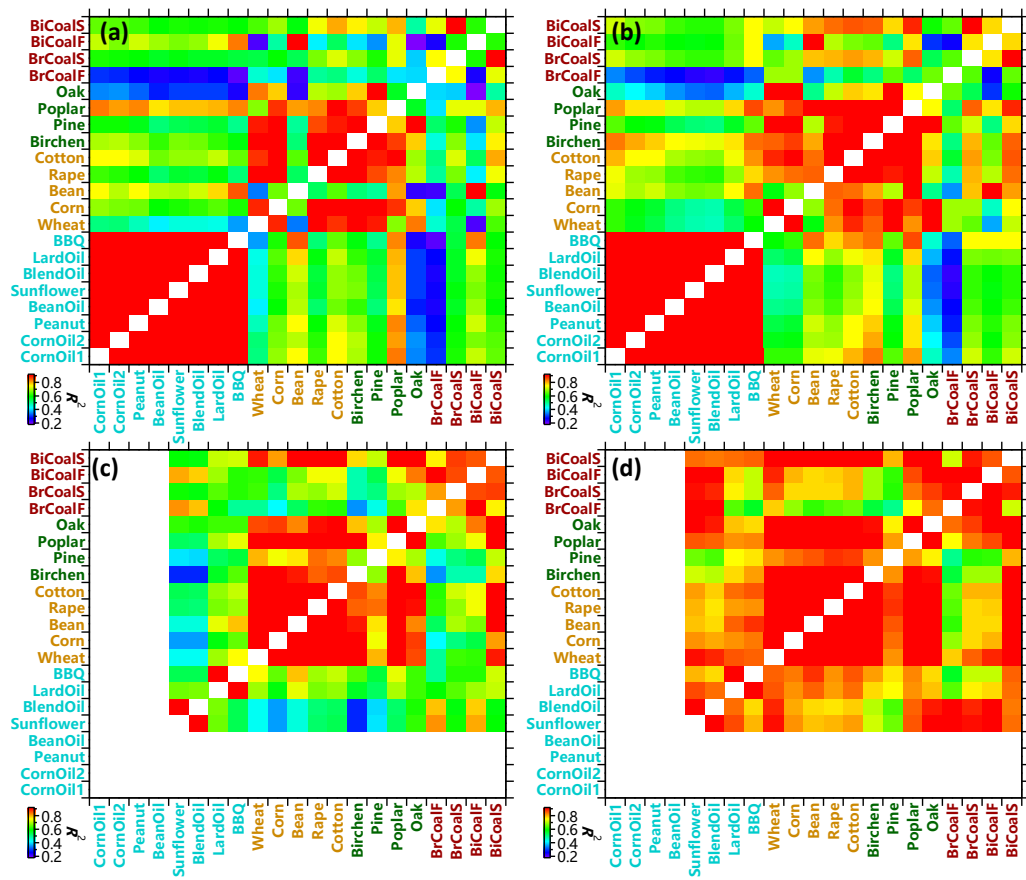
Figure 5.~~Figure 2.~~ **Mass spectral correlations of OA measured by (a) SV-AMS, (b) CV-ACSM, and WSOA measured by (c) SV-AMS and (d) CV-ACSM. The detailed descriptions of cooking and burning fuels are presented in Table ~~S1~~S3.**
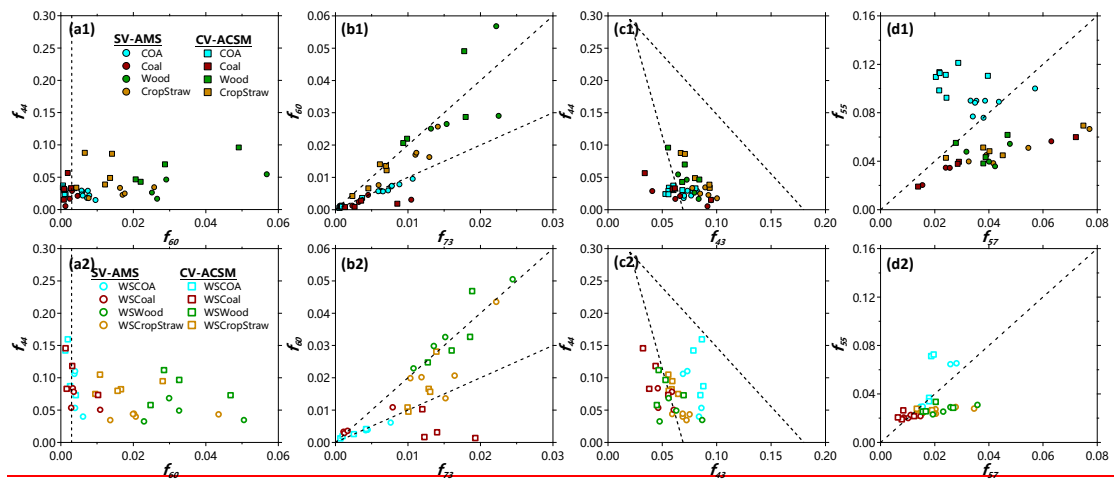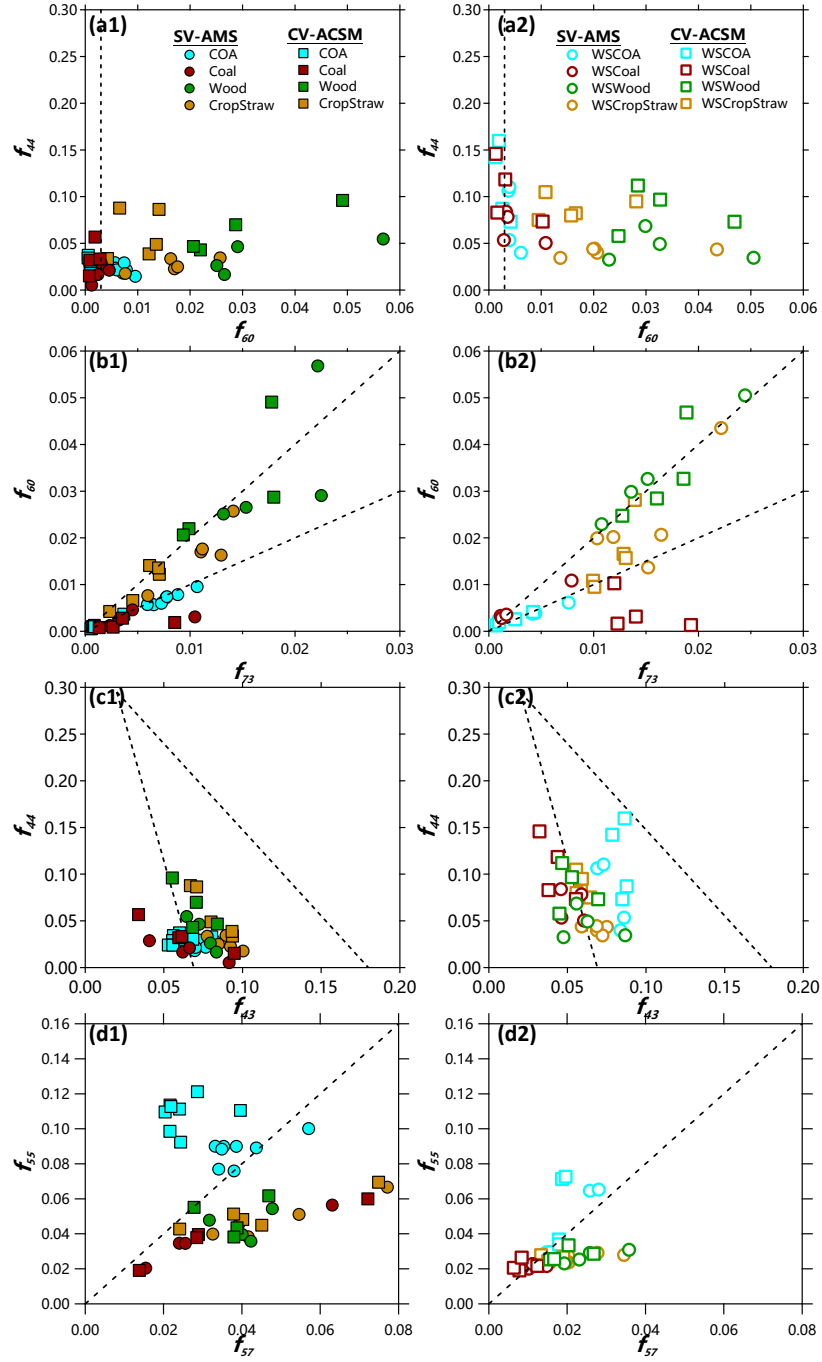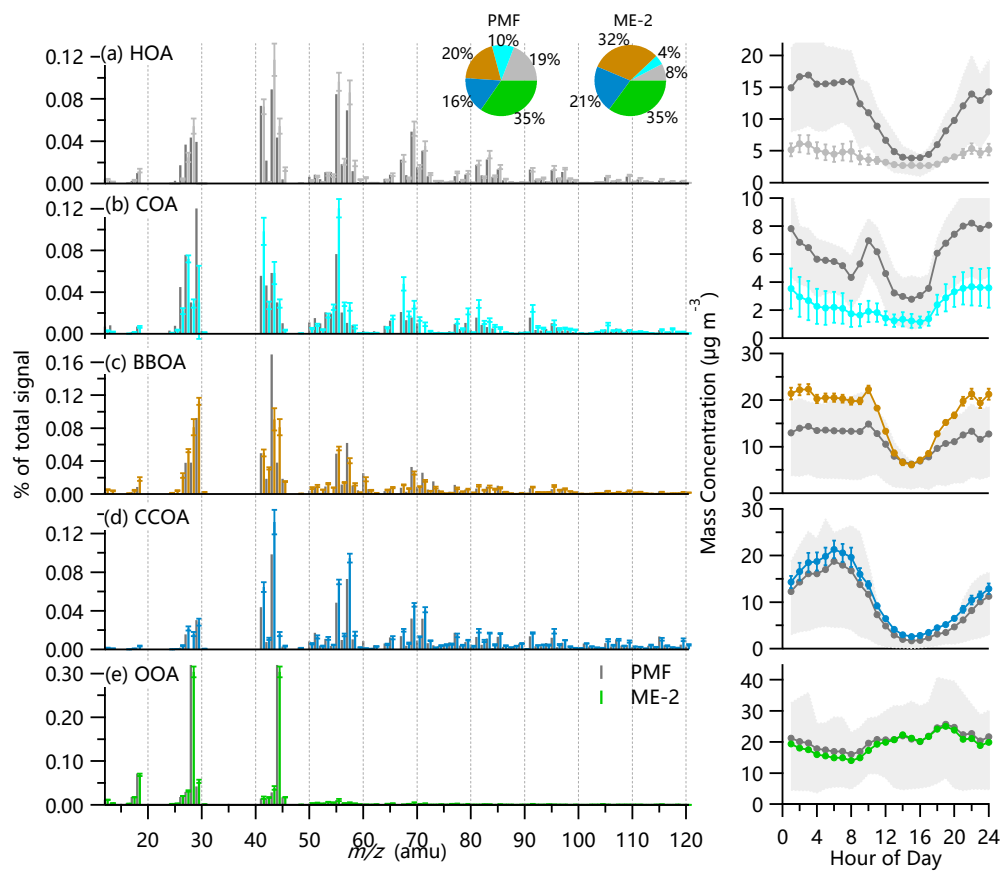
Figure 3~~6~~. Scatter plots of (a) f_{44} vs. f_{60}, (b) f_{60} vs. f_{73}, (c) f_{44} vs. f_{43} and (d) f_{55} vs. f_{57} for OA (top panel) and WSOA (bottom panel) from SV-AMS and CV-ACSM measurements.
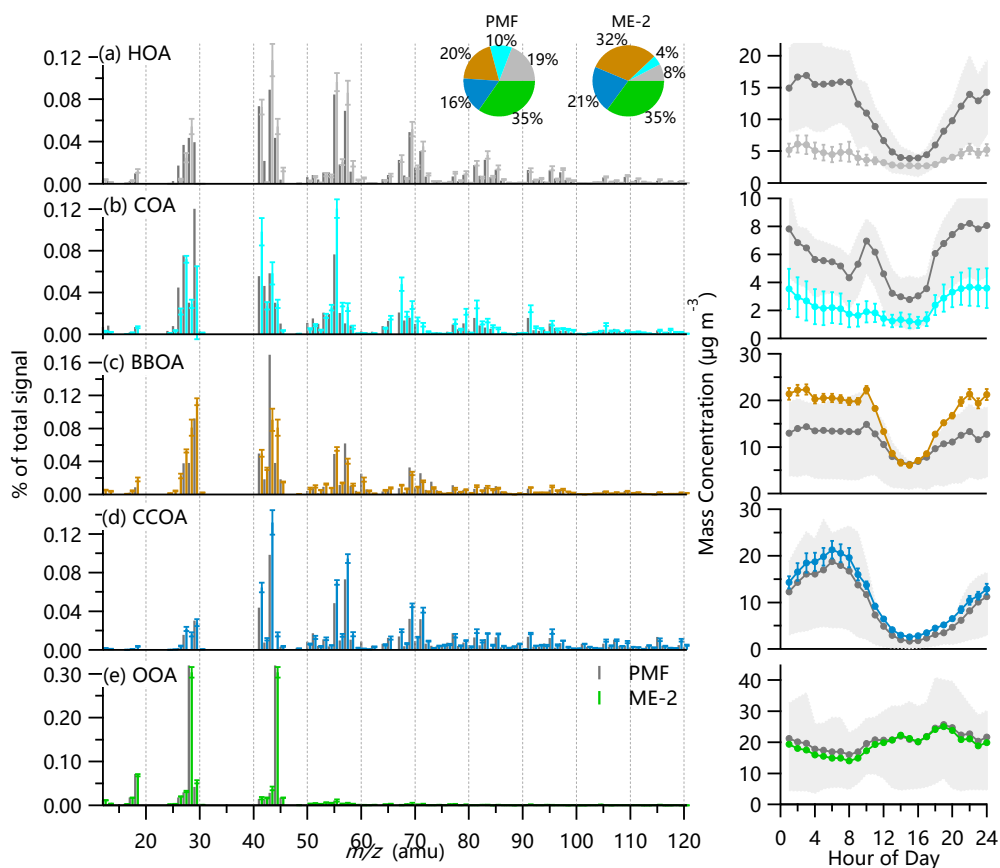
27

Figure 47. Comparisons of mass spectral profiles, diurnal cycles and compositions of five OA factors between PMF and ME-2 analysis at a rural site in North China Plain in winter. The ME-2 results are the averages with a-value ranging from 0 to 0.3, and the error bars are one standard deviations. The shaded areas in right panel indicate 25th and 75th percentiles of PMF results.